X–ray follow–up work on unassociated sources listed in the *INTEGRAL*/IBIS cat1000 catalogue:

Swift/XRT observations of objects already appearing in the 4th *INTEGRAL*/IBIS survey

Raffaella Landi & Loredana Bassani

Report n. 656/2015

June 2015

INAF/IASF Bologna

Introduction

In the following, we provide a report on a number of *Swift*/XRT observations performed so far on still unassociated sources listed in the new *INTEGRAL*/IBIS survey and also reported in the fourth one (Bird et al. 2010). Results on individual objects are presented and briefly discussed. Simple spectral fittings have been performed on the data to obtain information on the source spectrum only for those sources whose XRT data are of sufficient quality (typically > 50 counts in the source spectrum extraction region) to allow a reliable spectral analysis; quoted column densities are always in excess to the Galactic value in the source direction (Kalberla et al. 2005). In the images reported below, the black circle and the black–dotted circle depict the IBIS 90% and 99% positional uncertainty, respectively, as reported in the latest *INTEGRAL*/IBIS catalogue. Only X–ray detections above 2.5σ confidence level (c.l.) are reported and discussed.

The *INTEGRAL*/IBIS sources (names are from the new survey) discussed in this report, listed in order of increasing R.A., are the following:

- IGR J01085–4550 (Flag: WARN)
- IGR J03199+7402
- IGR J06552–1146
- IGR J08262+4051
- IGR J10200–1436
- IGR J11502–5427 (Flag: WARN)
- IGR J13045–5630
- IGR J13290–6323
- IGR J13396–3306
- IGR J14227–2931
- IGR J14297–5623
- IGR J14385+8553
- IGR J15077+0906
- IGR J16226–2759 (Flag: WARN)
- IGR J16327–4940
- IGR J16388+3557
- IGR J17468–2902 (Flags: BLEND, GCFlag2)
- IGR J17479–2807 (Flags: BLEND, GCFlag2)
- IGR J18175–1530
- IGR J19079+0942 (Flag: WARN)

- IGR J19113+1533
- IGR J19118+1125 (Flag: WARN)
- IGR J19294–1746 (Flag: WARN)
- IGR J19295–0919 (Flag: WARN)
- IGR J21268+6203 (Flag: WARN)
- IGR J21319+3619 (Flag: WARN)
- IGR J22014+6034
- IGR J22253+5046
- IGR J23070+2203

The multi–wavelength properties of the objects analysed in this work have been collected by exploiting various catalogues and databases reported in the following list:

- United States Naval Observatory B–1.0 catalogue (USNO B–1.0, Monet et al. 2003);
- United States Naval Observatory A–2.0 catalogue (USNO A–2.0, available at: `http://archive.eso.org/skycat/servers/usnoa/`);
- The Two Micron All–Sky Survey (2MASS, Skrutskie et al. 2006);
- Two Micron All Sky Survey Extended Source Survey (2MASX, Skrutskie et al. 2006);
- The Wide–field Infrared Survey Explorer (WISE, Wright et al. 2010);
- The *ROSAT* All–Sky Survey Bright/Faint Source Catalogues (Voges et al. 1999);
- The Galaxy Evolution Explorer All–Sky Survey (GALEX, Bianchi et al. (2011);
- Galactic Legacy Infrared Mid–Plane Survey Extraordinaire (GLIMPSE, available at: `http://vizier.u-strasbg.fr/viz-bin/VizieR?-source=II/293`;
- The Second Data Release of the INT Photometric H–Alpha Survey of the Northern Galactic Plane (IPHAS DR2, Barentsen et al. 2014);
- UKIRT Infrared Deep Sky Survey (UKIDSS) Galactic Plane Survey (GPS) (Lucas et al. 2008);
- CRATES: An All–Sky Survey of Flat–Spectrum Radio Sources (Healey et al. 2007);
- The National Radio Astronomy Observatory (NRAO) Very Large Array (VLA) Sky Survey (NVSS, Condon et al. 1998);
- The Million Quasars Catalog, Version 4.4, 6 February 2015 (MILLIQUAS, available at: `http://quasars.org/milliquas.htm`;
- The *XMM–Newton* Slew Survey Full Source Catalogue (XMMSL1, Saxton et al. 2008);

- The *XMM–Newton* Serendipitous Source Catalogue (3XMM–DR4, Watson et al. 2013);
- The Magellanic Quasars Survey (MQS, Kozlowski et al. 2013);
- The *Swift*/XRT Point Source Catalogue (1SXPS, Evans et al. 2014);
- The *Swift* Serendipitous Survey in deep XRT GRB fields (SwiftFT, Puccetti et al. 2011);
- The SIMBAD Astronomical Database (available at: `http://simbad.u-strasbg.fr/simbad/`;
- The NASA/IPAC Extragalactic Database (NED, available at: `https://ned.ipac.caltech.edu/`;
- The High Energy Astrophysics Science Archive Research Center provided by NASA's Goddard Space Flight Center (HEASARC, available at: `http://heasarc.gsfc.nasa.gov/`.

IGR J01085–4550

(IBIS detection: 246.5–day outburst)

Four XRT observations available:

1. obscode: 00045385001
   observation date: 08/03/2011
   exposure: 695 s

2. obscode: 00045385002
   observation date: 17/03/2011
   exposure: 923 s

3. obscode: 00045385004
   observation date: 25/03/2011
   exposure: 612 s

4. obscode: 00045385005
   observation date: 28/03/2011
   exposure: 3217 s

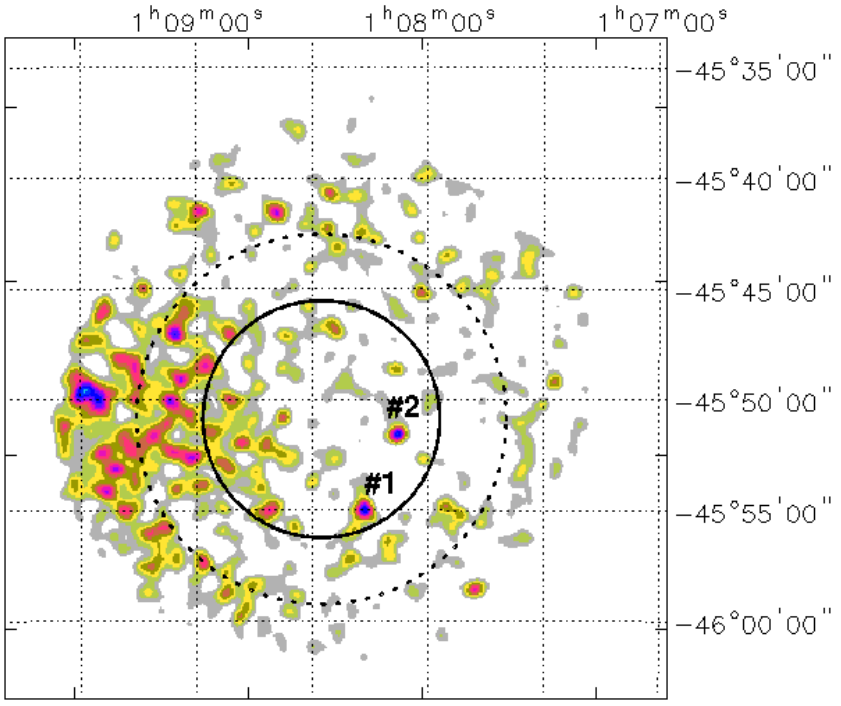

Figure 1: 0.3–10 keV XRT image of the IGR J01085–4550 field.

XRT detects two X–ray sources within the 90% IBIS positional uncertainty:

➢ Source #1 is located at:

R.A.(J2000) = $01^{\rm h}08^{\rm m}16'.20$

Dec.(J2000) = $-45^{\circ}54'55''.40$

error box = $6''.00$

It is detected at 2.5σ c.l. in the 0.3–10 keV energy band, and it is not visible above 3 keV.

No counterpart has been found to this XRT detection:

➢ Source #2 is located at:

R.A.(J2000) = $01^{\rm h}08^{\rm m}07'.60$

Dec.(J2000) = $-45^{\circ}51'33''.70$

error box = $6''.00$

It is detected at 2.6σ in the 0.3–10 keV energy range, but not above 3 keV.

Multi–wavelength counterparts to this XRT detection:

- USNO–A2.0 U0375.00346030 with magnitudes $R = 17.6$, and $B = 19.4$;
- GALEXASC J010807.61–455132.7.

IGR J03199+7402

(IBIS detection: persistent)

Two XRT observations available:

1. obscode: 00041196001
   observation date: 15/10/2010
   exposure: 3337 s
2. obscode: 00041196002
   observation date: 18/10/2010
   exposure: 1707 s

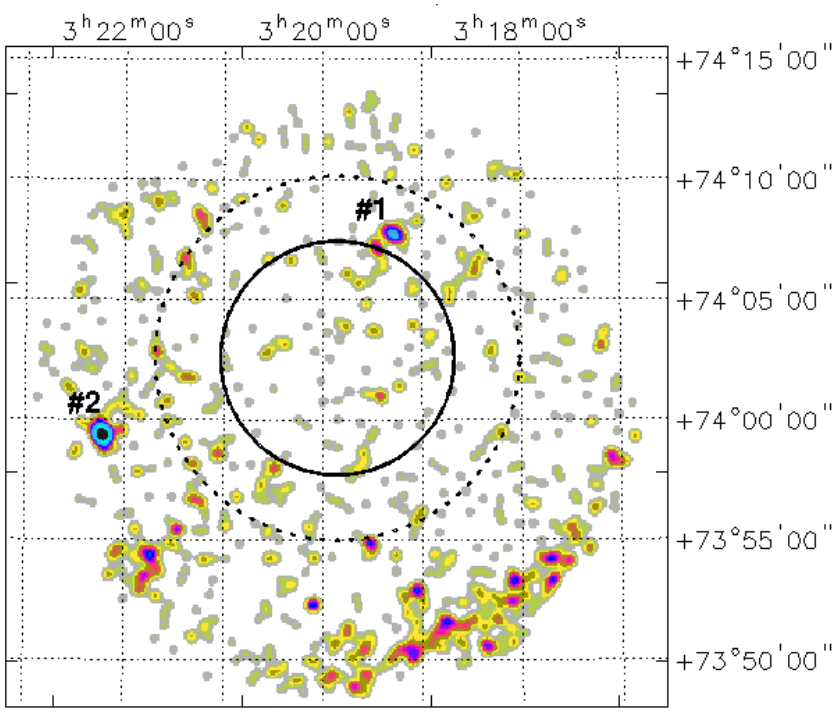

Figure 2: 0.3–10 keV XRT image of the IGR J03199+7402 field.

XRT detects two X–ray sources in the region surrounding IGR J03199+7402:

➢ Source #1 is located within the 99% IBIS positional uncertainty at:

R.A.(J2000) = $03^h19^m16'.80$

Dec.(J2000) = $+74°07'42''.70$

error box = $6''.00$

It is detected at 3.1σ c.l. in the 0.3–10 keV energy band, but it is not revealed above 3 keV.

Multi–wavelength counterparts to this XRT detection:

- USNO–A2.0 U1575.01658513 with magnitudes $R = 16.6$, and $B = 17.6$;
- 2MASS J03191639+7407420 with magnitudes $J = 15.524 \pm 0.072$, $H = 15.231 \pm 0.111$, and $K = 15.214 \pm 0.0211$;
- WISE J031916.30+740742.1 with colours $W1 = 15.064 \pm 0.039$, $W2 = 14.941 \pm 0.080$, $W3 = 12.741 \pm 0.484$, and $W4 = 8.770 \pm 0.000$;
- 1SXPS J031916.1+740741.

Because of the low statistical quality of the data, we can infer a 2–10 keV flux of $\sim 2 \times 10^{-13}$ erg cm^{-2} s^{-1} by assuming a power law passing through Galactic absorption ($N_{\rm H(Gal)} = 1.79 \times 10^{21}$ cm^{-2}) and freezing the photon index to 1.8.

➢ Source #2 falls outside the 99% IBIS error circle and is located at:

R.A.(J2000) = $03^{\rm h}22^{\rm m}13'.68$

Dec.(J2000) = $+73^{\circ}59'25''.21$

error box = $4''.80$

It is detected at 6.6σ c.l. in the 0.3–10 keV energy range, but it is not visible above 3 keV.

Multi–wavelength counterparts to this XRT detection:

- USNO–A2.0 U1575.01674673 with magnitudes $R = 11.2$, and $B = 12.5$;
- 2MASS J03221301+7359249 with magnitudes $J = 9.011 \pm 0.020$, $H = 8.401 \pm 0.021$, and $K = 8.254 \pm 0.019$;
- WISE J032213.01+735924.9 with colours $W1 = 8.186 \pm 0.024$, $W2 = 8.239 \pm 0.020$, $W3 = 8.107 \pm 0.018$, and $W4 = 8.348 \pm 0.208$;
- 1SXPS J032213.2+735923;
- Star TYC 4338–668–1 of spectral type rK3 III.

Also in this case due to the low quality of the XRT data we can only estimate a 2–10 keV flux of $\sim 2 \times 10^{-13}$ erg cm^{-2} s^{-1} by modelling the XRT data with a bremsstrahlung model ($kT \sim 1.5$ keV) passing through Galactic absorption ($N_{\rm H(Gal)} = 1.76 \times 10^{21}$ cm^{-2}).

The overall properties of the XRT detections lead us to conclude that none of them are convincing: source #1 is too dim and soft to be a likely counterpart, while source #2 is a simple star unlikely to emit high–energy photons.

IGR J06552–1146

(IBIS detection: 1611.4–day outburst)

Three XRT observations available:

1. obscode: 00041201001
   observation date: 29/09/2010
   exposure: 275 s

2. obscode: 00041201002
   observation date: 07/02/2011
   exposure: 468 s

3. obscode: 00041201003
   observation date: 11/02/2011
   exposure: 4449 s

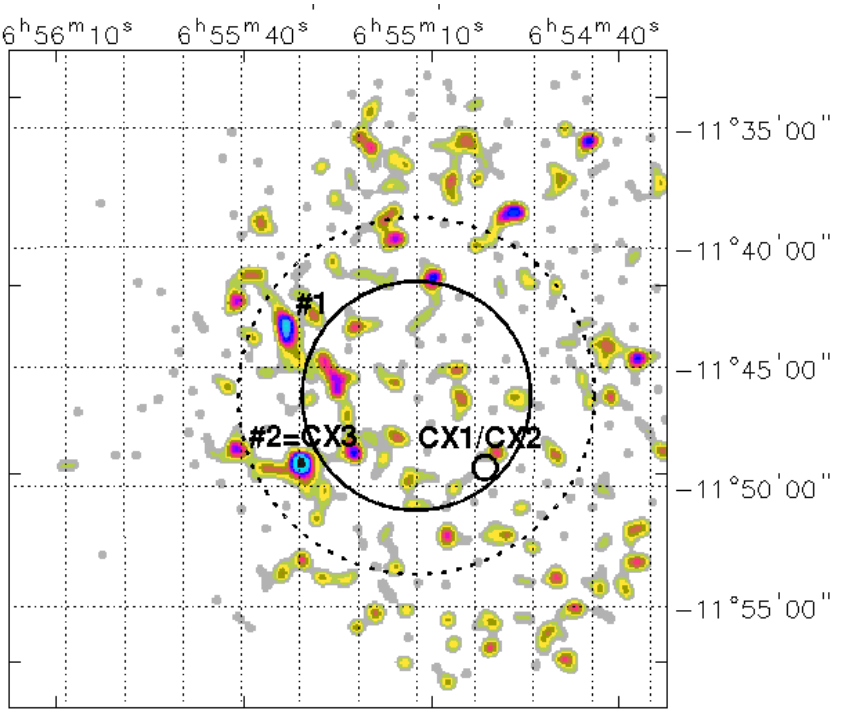

Figure 3: 0.3–10 keV XRT image of the IGR J06552–1146 field. We also plot the position of the three sources detected by *Chandra*: CX1 and CX2 which cannot be resolved by XRT (small black circle), and CX3 which coincides with our source #2 (see Arabaci et al. 2012).

XRT detects two X–ray objects whose positions are compatible with the 99% IBIS error circles:

➢ Source #1 is located at:

R.A.(J2000) = $06^{h}55^{m}32'.30$

Dec.(J2000) = $-11^{\circ}43'11''.10$

error box = $6''.00$

It is detected at 2.3σ c.l. in the 0.3–10 keV energy range, and it is not visible above 3 keV.

No counterpart has been found to this XRT detection.

➢ Source #2 is located at:

R.A.(J2000) = $06^{h}55^{m}29'.80$

Dec.(J2000) = $-11^{\circ}49'01''.10$

error box = $6''.00$

It is detected at 2.8σ c.l. in the 0.3–10 keV energy range, but it is not visible above 3 keV.

Multi–wavelength counterparts to this XRT detection:

- WISE J065529.52–114859.8 with colours $W1 = 15.404 \pm 0.052$, $W2 = 14.424 \pm 0.070$, $W3 = 10.913 \pm 0.096$, and $W4 = 9.050 \pm 0.491$;
- CXOU J065529.5–114900 (see Arabaci et al. 2012);
- 1SXPS J065529.8–114900.

This IBIS source has already been studied by means of *Chandra* observations by Arabaci et al. (2012). The authors detected three sources of which two are inside the IBIS error circle and one (their source #3) coincides with our source #2. Their source #1 is an active star (spectral type K5–8 Ve) possibly of the RS CV class.

The overall properties of both of the X–ray detections make unlikely their association with the IBIS emitter.

IGR J08262+4051

(IBIS detection: 2.3–day outburst)

Seven XRT observations available:

1. obscode: 00031311001
   observation date: 16/12/2008
   exposure: 5272 s
2. obscode: 00031311002
   observation date: 17/12/2008
   exposure: 4959 s
3. obscode: 00031311003
   observation date: 23/12/2008
   exposure: 8655 s
4. obscode: 00031311004
   observation date: 30/12/2008
   exposure: 5182 s
5. obscode: 00031311005
   observation date: 31/12/2008
   exposure: 980 s
6. obscode: 00031311006
   observation date: 06/01/2009
   exposure: 4039 s
7. obscode: 00031311007
   observation date: 07/01/2009
   exposure: 6201 s

This source has already been discussed by Landi et al. (2010). Here, we provide evidence for the presence of two extra sources within both the 90% and 99% IBIS positional uncertainties.

As can be seen from Figure 4, the region surrounding the IBIS source is very crowded because of the presence of the Cluster of galaxies SDSS–C4–DR3 3247, located just outside the 99% IBIS error circle. Given the variability of the gamma–ray source, it is unlikely that the cluster is responsible for the IBIS emission; besides, its spectrum is very soft disappearing above 2–3 keV. Therefore, in the following we discuss and show in Figure 4, only those X–ray sources, whose position are compatible with either the 90% or the 99% IBIS positional uncertainties, which are still detected above 3 keV:

➢ Source #1 lies within the 90% IBIS error circle and is located at:

R.A.(J2000) = $08^{h}26^{m}17'.99$

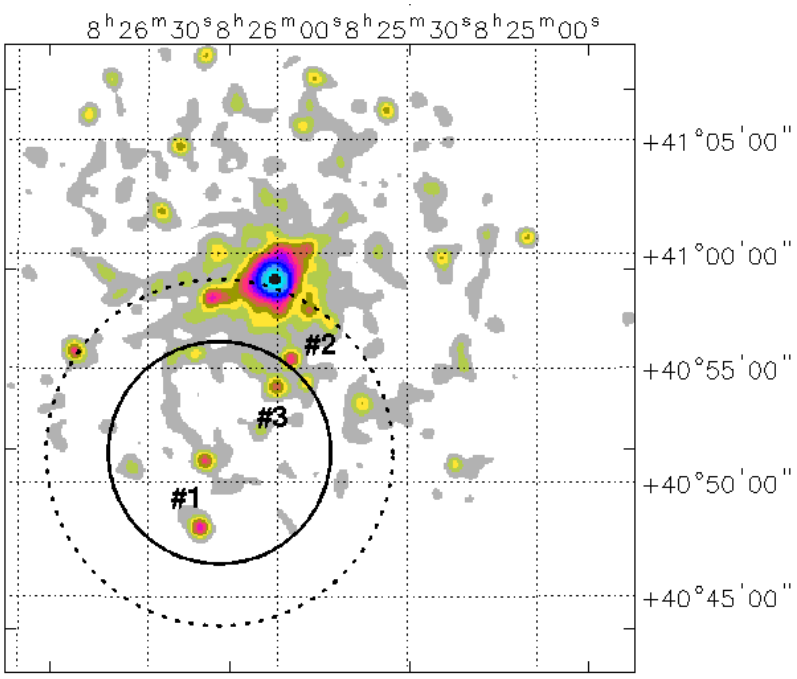

Figure 4: 0.3–10 keV XRT image of the IGR J08262+4051 field.

Dec.(J2000) = $+40°48'02''.60$

error box = $4''.37$

It is detected at 5.9σ c.l. in the 0.3–10 keV energy band, and it is still observed above 3 keV at 2.8σ c.l.

Multi–wavelength counterparts to this XRT detection:

- USNO–A2.0 U1275.07272622 with magnitudes $R = 19.5$, and $B = 19.8$;
- WISE J082617.93+404758.5 with colours $W1 = 16.736 \pm 0.127$, $W2 = 15.323 \pm 0.126$, $W3 = 12.376 \pm 0.385$, and $W4 = 8.562 \pm 0.000$;
- SDSS J082617.87+404758.6 (type 1 QSO, $z = 0.975000$, Masetti et al. 2012);
- 1SXPS J082617.6+404756 (6.7 arcseconds away from the XRT centroid).

A simple power law passing through Galactic absorption ($N_{\rm H(Gal)} = 4.06 \times 10^{20}$ cm^{-2}) provides a photon index $\Gamma = (1.34 \pm 0.73)$ and a 2–10 keV flux around 7×10^{-14} erg cm^{-2} s^{-1}.

➢ Source #2 is detected within the 99% IBIS error circle at:

R.A.(J2000) = $08^{\rm h}25^{\rm m}56'.80$

Dec.(J2000) = $+40°55'21''.80$

error box = $6''.00$

It is detected at 5.0σ and 3.6σ c.l. in 0.3–10 keV energy band and above 3 keV, respectively.

Multi–wavelength counterparts to this XRT detection:

- 1SXPS J082556.6+405519.

➢ Source #3 lies within the 90% IBIS error circle and is located at:

R.A.(J2000) = $08^{\rm h}25^{\rm m}59'.70$

Dec.(J2000) = $+40^{\circ}54'08''.20$

error box = $6''.00$

It is detected at 5.0σ and 2.8σ c.l. in the 0.3–10 keV energy band and above 3 keV, respectively.

Multi–wavelength counterparts to this XRT detection:

- USNO–A2.0 U1275.07271122 with magnitudes $R = 19.1$, and $B = 19.8$;
- WISE J082600.28+405408.8 with colours $W1 = 15.268 \pm 0.045$, $W2 = 14.778 \pm 0.084$, $W3 = 12.043 \pm 0.000$, and $W4 = 9.023 \pm 0.000$ (6.7 arcseconds away from the XRT centroid);
- SDSS J082559.64+405405.4 (extended source);
- 1SXPS J082600.0+405405;
- Candidate AGN object from SDSS–DR4 at $z = 0.25221$ (Cavuoti et al. 2014).

On the basis of the properties acquired for the XRT detections, we propose the identification/classification suggested by Masetti et al. (2012) as the most likely, although optical spectroscopy of source #1 and #2 are encouraged to exclude their possible association with the IBIS source.

IGR J10200–1436

(IBIS detection: persistent)

Two XRT observations available:

1. obscode: 00045394001
   observation date: 24/03/2011
   exposure: 1479 s

2. obscode: 00045394002
   observation date: 24/03/2011
   exposure: 2840 s

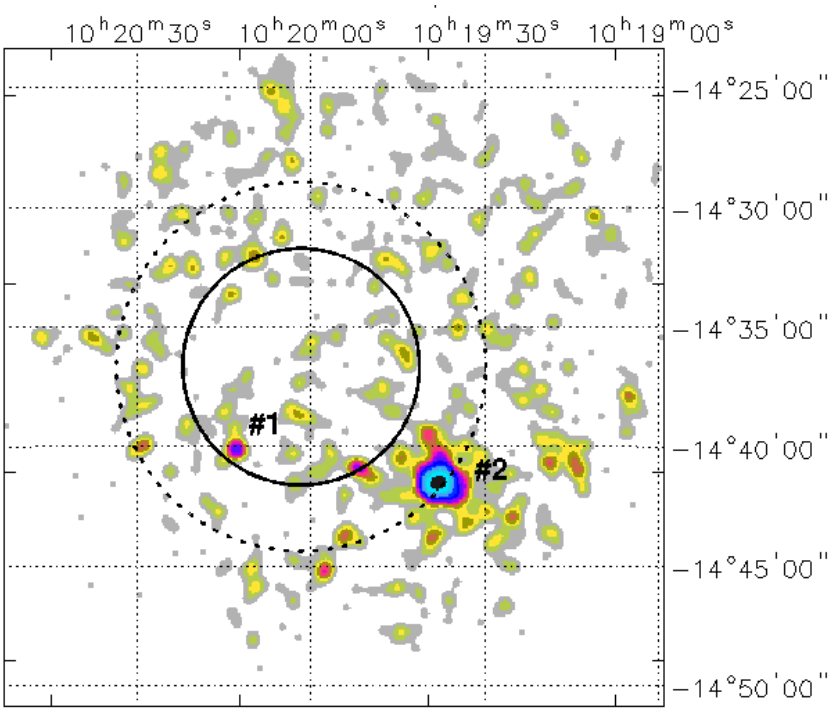

Figure 5: 0.3–10 keV XRT image of the IGR J10200–1436 field.

XRT detects two X–ray objects whose positions are compatible with either the 90% or the 99% IBIS error circles:

➢ Source #1, which lies inside the 90% IBIS error circle, is located at:

R.A.(J2000) = $10^{h}20^{m}12'.80$

Dec.(J2000) = $-14°40'06''.60$

error box = $6''.00$

It is detected at 2.4σ c.l. in the 0.3–10 keV energy band; no detection above 3 keV.

Multi–wavelength counterparts to this XRT detection:

- USNO–A2.0 U0750.07216191 with magnitudes $R = 13.1$, and $B = 14.1$;
- 2MASS J10201268–1440108 with magnitudes $J = 11.671 \pm 0.024$, $H = 11.136 \pm 0.023$, and $K = 11.019 \pm 0.023$;
- WISE J102012.63–144010.4 with magnitudes $W1 = 10.936 \pm 0.022$, $W2 = 10.951 \pm 0.022$, $W3 = 10.884 \pm 0.093$, and $W4 = 9.167 \pm 0.000$;
- 1SXPS J102012.8–144004.

The faintness of this source does not allow us to perform a reliable spectral analysis.

➢ Source #2, which lies at the border of the 99% IBIS error circle, is located at:

R.A.(J2000) = $10^{\rm h}19^{\rm m}37'.99$

Dec.(J2000) = $-14^\circ 41' 29''.91$

error box = $4''.25$

It is detected at 8.5σ c.l. in the 0.3–10 keV energy band, but it is not revealed above 3 keV.

Multi–wavelength counterparts to this XRT detection:

- USNO–B1.0 0753–0234945 with magnitudes $R1 = 18.70$, $R2 = 17.99$, and $B2 = 20.85$;
- WISE J101938.39–144128.9 with colours $W1 = 16.689 \pm 0.122$, $W2 = 16.469 \pm 0.337$, $W3 = 12.764 \pm 0.000$, and $W4 = 9.202 \pm 0.000$;
- 1SXPS J101937.5–144126.

This object was classified as XBONG ($z = 0.391$) by Masetti et al. (2013).
The X–ray data are modelled with a simple power law ($N_{\rm H(\mathit{Gal})} = 6.64 \times 10^{20}$ cm^{-2}), with a photon index $\Gamma = \left(1.60^{+0.40}_{-0.42}\right)$ and a 2–10 keV flux of $\sim 8 \times 10^{-13}$ erg cm^{-2} s^{-1}.

For this IBIS source, the XRT follow–up observations lead us to confirm the association/identification proposed by Masetti et al. (2012), although the source now lies at the border of the 99% IBIS error circle.

IGR J11502–5427

(IBIS detection: 1.1–day outburst)

Two XRT observations available:

1. obscode: 00041204001
   observation date: 25/03/2010
   exposure: 4071 s

2. obscode: 00041204002
   observation date: 11/04/2010
   exposure: 189 s

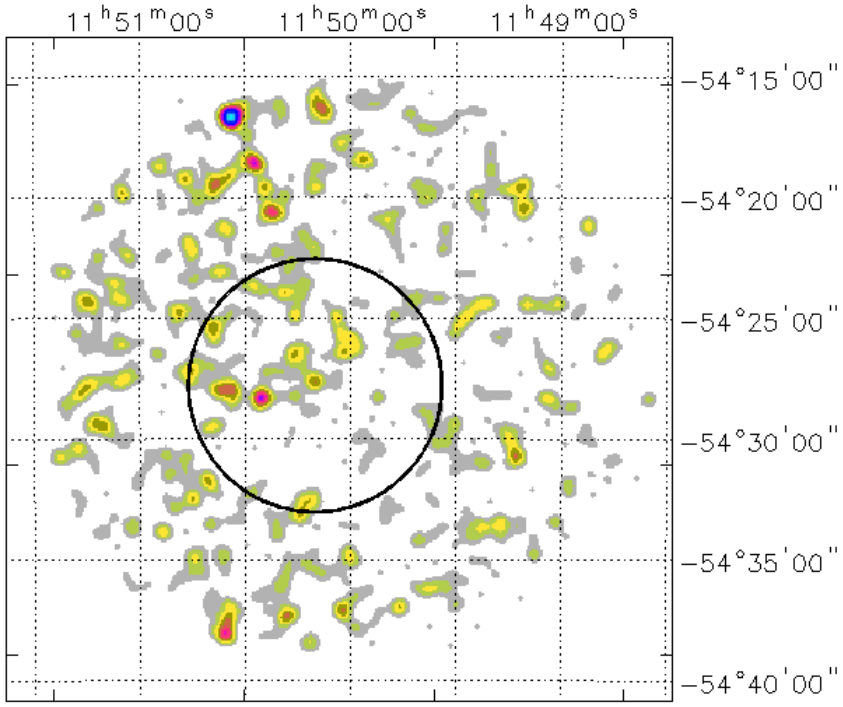

Figure 6: 0.3–10 keV XRT image of the IGR J11502–5427 field.

No source has been detected by XRT within the IBIS error circle, but this is not surprising giving the extreme variability of the IBIS source.

IGR J13045–5630

(IBIS detection: persistent)

Five XRT observations available:

1. obscode: 00041206001
   observation date: 18/03/2010
   exposure: 1723 s
2. obscode: 00041206001
   observation date: 19/02/2011
   exposure: 1647 s
3. obscode: 00041206003
   observation date: 20/02/2011
   exposure: 1043 s
4. obscode: 00032118001
   observation date: 11/10/2011
   exposure: 1003 s
5. obscode: 00032118002
   observation date: 18/10/2011
   exposure: 932 s

XRT detects only one source, whose position is compatible with the 90% IBIS positional uncertainty, which is located at:

R.A.(J2000) = $13^{\rm h}04^{\rm m}31'.57$

Dec.(J2000) = $-56^\circ30'55''.88$

error box = $4''.52$

It is detected at 7.4σ and 7.1σ c.l. in the 0.3–10 keV energy range and above 3 keV, respectively.

The counterparts to this X–ray object are discussed by Rodriguez et al. (2010). We provide an enhancement of the source position and error box by summing all the XRT observations available in the archive. By adopting the enhanced coordinates we pinpoint a single optical counterpart and provide further associations from various databases:

- USNO–A2.0 0300.17436154 with magnitudes $R = 12.2$, and $B = 15.3$;
- 2MASS 13043169–5630595 with magnitudes $J = 12.668 \pm 0.000$, $H = 11.987 \pm 0.000$, and $K = 11.911 \pm 0.054$;
- WISE J130431.77–563058.4 with colours $W1 = 10.464 \pm 0.022$, $W2 = 9.497 \pm 0.021$, $W3 = 6.214 \pm 0.014$, and $W4 = 3.436 \pm 0.017$;

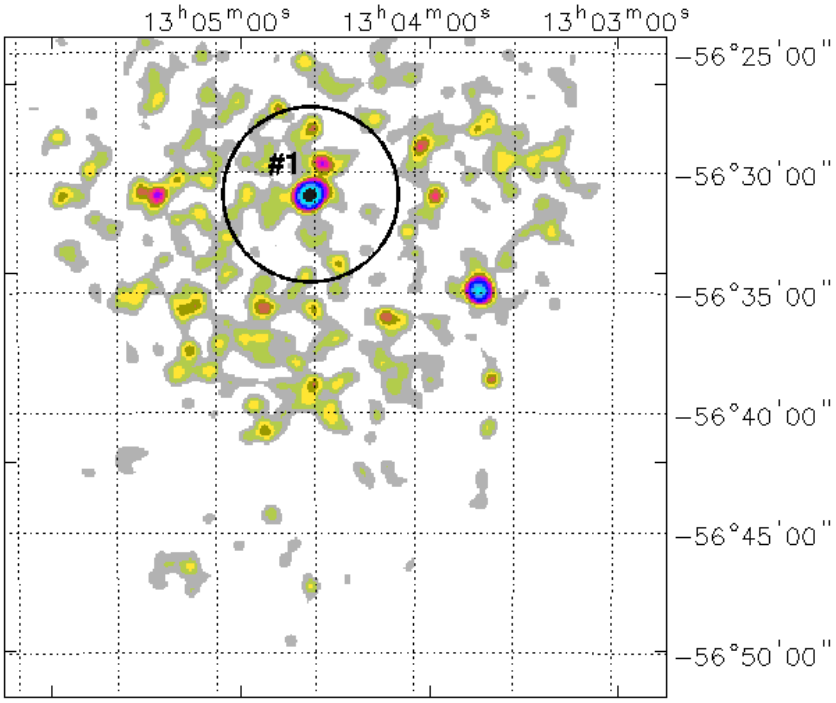

Figure 7: 0.3–10 keV XRT image of the IGR J13045–5630 field.

- 1SXPS J130431.5–563057.

IGR J13290–6323

(IBIS detection: 3.1–day outburst)

One XRT observation available:

1. obscode: 00042205001
   observation date: 25/02/2011
   exposure: 479 s

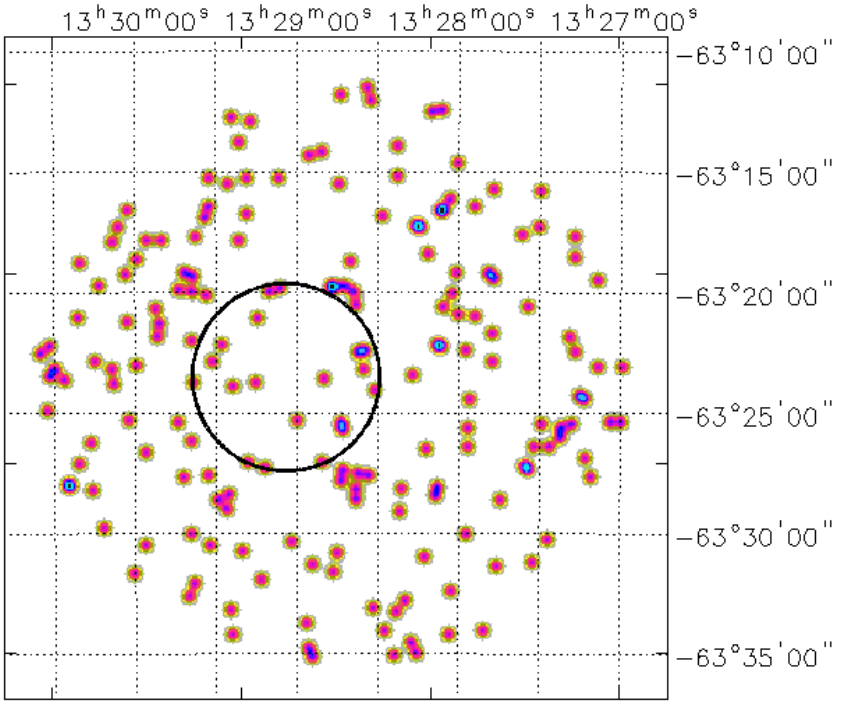

Figure 8: 0.3–10 keV XRT image of the IGR J13290–6323 field.

No source has been detected by XRT within the IBIS error circle, probably due to the low exposure.

IGR J13396–3306

(IBIS detection: 1550.4–day outburst)

Three XRT observations available:

1. obscode: 00041208001
   observation date: 09/05/2013
   exposure: 271 s

2. obscode: 00041208002
   observation date: 23/09/2013
   exposure: 236 s

3. obscode: 00041208003
   observation date: 10/05/2014
   exposure: 168 s

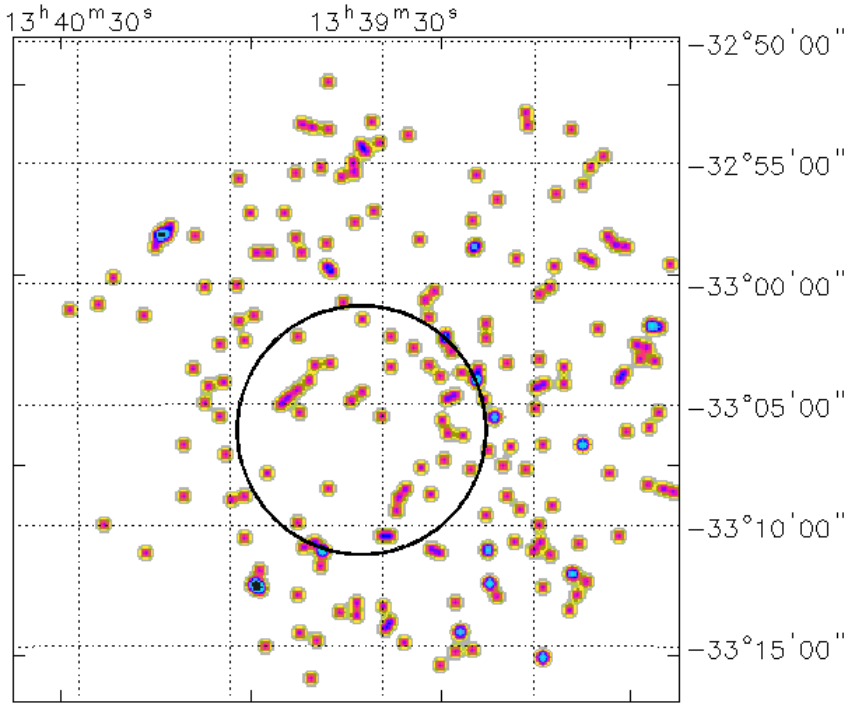

Figure 9: 0.3–10 keV XRT image of the IGR J13396–3306 field.

No source has been detected by XRT within the IBIS error circle, probably due to the low exposure.

IGR J14227–2931

(IBIS detection: 1246.6–day outburst)

One XRT observation available:

1. obscode: 00041211001
   observation date: 17/09/2010
   exposure: 4840 s

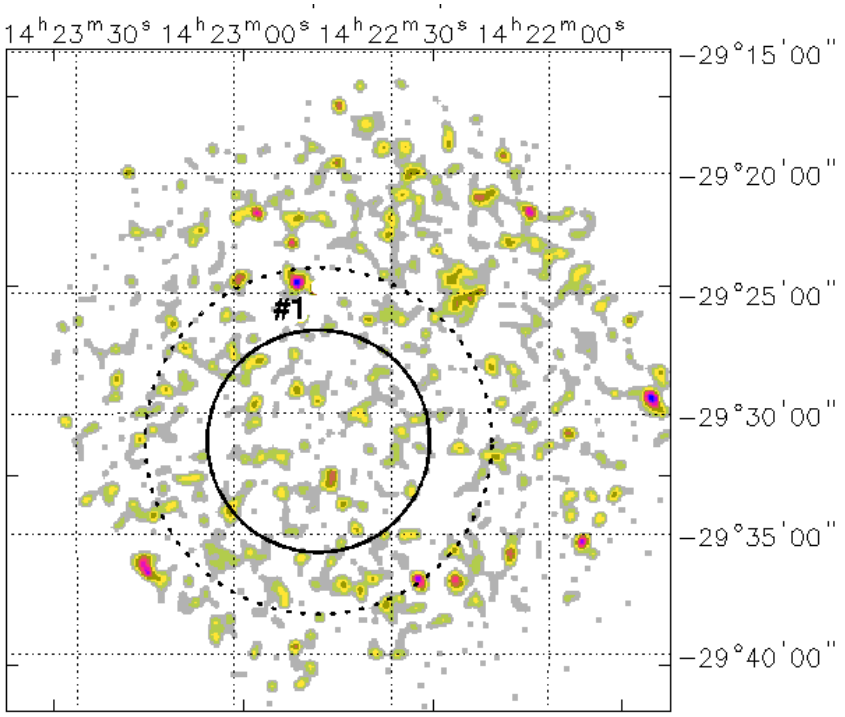

Figure 10: 0.3–10 keV XRT image of the IGR J14227–2931 field.

There is only one X–ray source detected within the 99% IBIS error circle located at:

R.A.(J2000) = $14^{h}22^{m}47'.90$

Dec.(J2000) = $-29^{\circ}24'35''.10$

error box = $6''.00$

It is detected at 2.5σ in the 0.3–10 keV energy range, and it is not revealed above 3 keV.

Multi–wavelength counterparts to this XRT detection:

- USNO–A2.0 U0600.16695864 with magnitudes $R = 18.1$, and $B = 19.3$;

- WISE J142248.16–292431.9 with colours $W1 = 14.788 \pm 0.034$, $W2 = 14.187 \pm 0.049$, $W3 = 11.306 \pm 0.118$, and $W4 = 8.694 \pm 0.000$;
- J142248.1–292432 listed in the MILLIQUAS catalogue;
- 1SXPS J142248.1–292432.

IGR J14297–5623

(IBIS detection: 1.5–day outburst)

One XRT observation available:

1. obscode: 00032484001
   observation date: 08/06/2012
   exposure: 2555 s

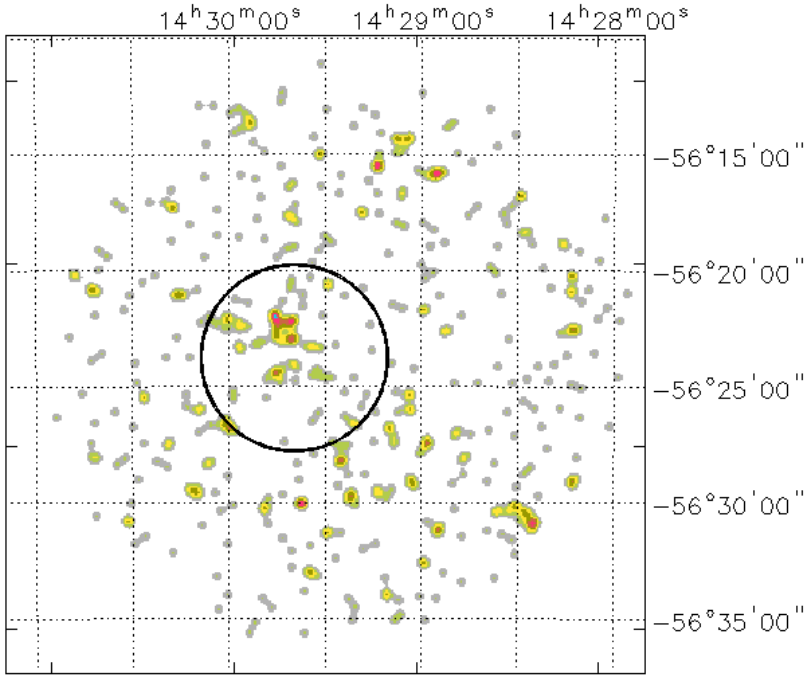

Figure 11: 0.3–10 keV XRT image of the IGR J14297–5623 field.

No X–ray source has been found within the IBIS error circle, but in this case variability might be an issue.

IGR J14385+8553

(IBIS detection: 64.3–day outburst)

Three XRT observations available:

1. obscode: 00041214001
   observation date: 01/04/2010
   exposure: 1964 s
2. obscode: 00041214002
   observation date: 02/04/2010
   exposure: 929 s
3. obscode: 00041214003
   observation date: 05/04/2010
   exposure: 2151 s

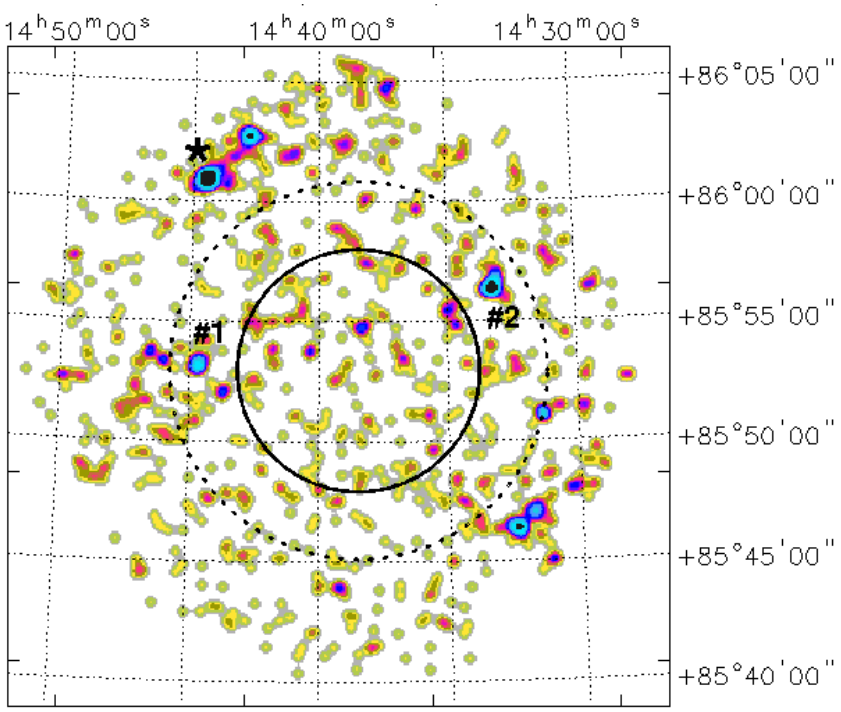

Figure 12: 0.3–10 keV XRT image of the IGR J14385+8553 field. The source flagged with an asterisk is the X–ray source proposed as a tentative counterpart to the IBIS object (Masetti et al. 2012).

XRT detects two X–ray sources within the 99% IBIS positional uncertainty:

➢ Source #1 is located at:

R.A.(J2000) = $14^{h}44^{m}37'.30$

Dec.(J2000) = $+85^{\circ}53'12''.00$

error box = $6''.00$

It is detected at 3.8σ in the 0.3–10 keV energy range, and it is not revealed above 3 keV.

Multi–wavelength counterparts to this XRT detection:

- USNO–B1.0 1758–0024901 with magnitudes $R2 = 19.59$, $B1 = 20.96$, and $B2 = 20.71$;
- WISE J144440.28+855315.2 with colours $W1 = 15.720 \pm 0.038$, $W2 = 14.960 \pm 0.051$, $W3 = 12.963 \pm 0.356$, and $W4 = 9.819 \pm 0.000$;
- 1SXPS J144439.7+855307 also listed as J144439.0+855310 in the MILLIQUAS catalogue.

From the XRT data we can only infer a 2–10 keV flux of $\sim 8 \times 10^{-14}$ erg cm^{-2} s^{-1} by assuming a power law continuum (photon index frozen to 1.8) passing through the Galactic absorption ($N_{\rm H(Gal)} = 5.37 \times 10^{20}$ cm^{-2}).

➢ Source #2 is located at:

R.A.(J2000) = $14^{\rm h}33^{\rm m}14'.80$

Dec.(J2000) = $+85^{\circ}56'21''.50$

error box = $6''.00$

It is detected at 5.4σ in the 0.3–10 keV energy range, and it is not revealed above 3 keV.

Multi–wavelength counterparts to this XRT detection:

- USNO–A2.0 U1725.00483988 ($R = 6.8$, and $B = 8.1$), USNO–A2.0 U1725.00484002 ($R = 11.3$, and $B = 8.0$), and USNO–A2.0 U1725.00484016 ($R = 7.3$, and $B = 0.0$);
- 2MASS J14331766+8556184 with magnitudes $J = 5.461 \pm 0.030$, $H = 5.021 \pm 0.016$, and $K = 4.886 \pm 0.023$;
- WISE J143317.49+855618.0 with colours $W1 = 4.816 \pm 0.077$, $W2 = 4.606 \pm 0.037$, $W3 = 4.843 \pm 0.014$, and $W4 = 4.760 \pm 0.023$;
- 1SXPS J143316.9+855618;
- Double or multiple star CCDM J14333+8556AB of spectral type K0 D.

Also in this case from the X–ray data we can only infer a 2–10 keV flux of $\sim 1.2 \times 10^{-13}$ erg cm^{-2} s^{-1} by assuming a power law continuum (photon index frozen to 1.8) passing through the Galactic absorption ($N_{\rm H(Gal)} = 5.44 \times 10^{20}$ cm^{-2}).

The asterisk in Figure 12 depicts the position of the source proposed by Masetti et al. (2012) as the tentative counterpart to IGR J14385+8553. It has been classified as a Seyfert 1.5 galaxy on

the basis of its optical spectrum. This source is detected by XRT at 6.9σ c.l. in the 0.3–10 keV energy range and it is still visible above 3 keV at 2.6σ c.l. Although this object lies outside the IBIS positional uncertainty, it is the hardest of the XRT detections, which may reinforce the suggestion by Masetti et al. (2012).

The XRT data are well modelled with a simple power law passing through the Galactic absorption ($N_{\rm H(Gal)} = 5.50 \times 10^{20}$ cm^{-2}) and having a photon index $\Gamma = (1.45 \pm 0.49)$ and a 2–10 keV flux of $\sim 5 \times 10^{-13}$ erg cm^{-2} s^{-1}.

IGR J15077+0906

(IBIS detection: 899.9–day outburst)

Four XRT observations available:

1. obscode: 00041218001
   observation date: 10/04/2011
   exposure: 150 s
2. obscode: 00041218002
   observation date: 18/06/2011
   exposure: 1013 s
3. obscode: 00041218001
   observation date: 18/12/2014
   exposure: 396 s
4. obscode: 00041218004
   observation date: 19/12/2014
   exposure: 891 s

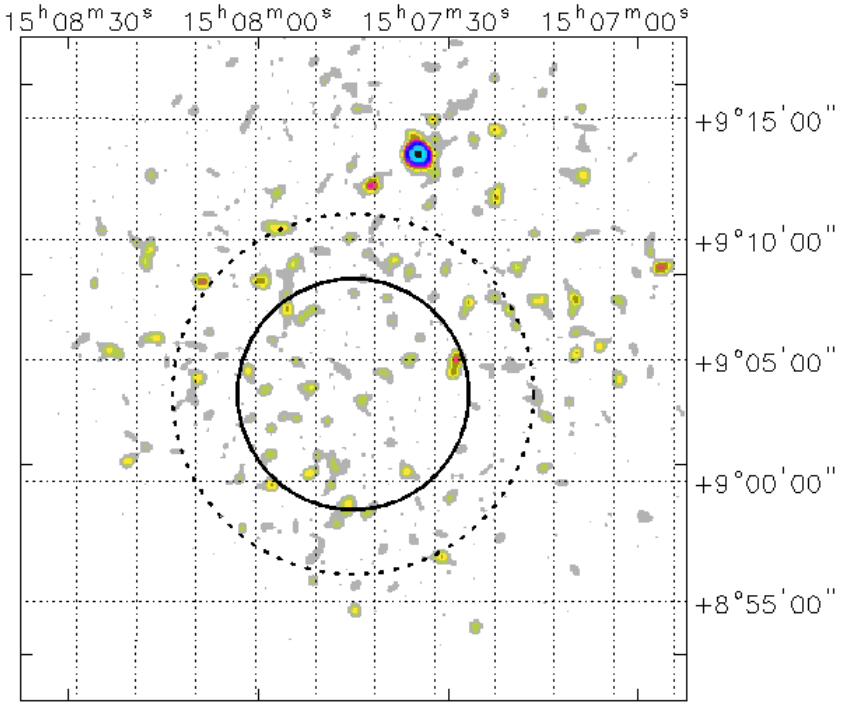

Figure 13: 0.3–10 keV XRT image of the IGR J15077+0906 field.

No source has been detected by XRT within both the 90% and 99% IBIS error circles.

IGR J16226–2759

(IBIS detection: 3.3–day outburst)

Two XRT observations available:

1. obscode: 00032485001
   observation date: 12/06/2012
   exposure: 2370 s

2. obscode: 00032485002
   observation date: 19/06/2012
   exposure: 2829 s

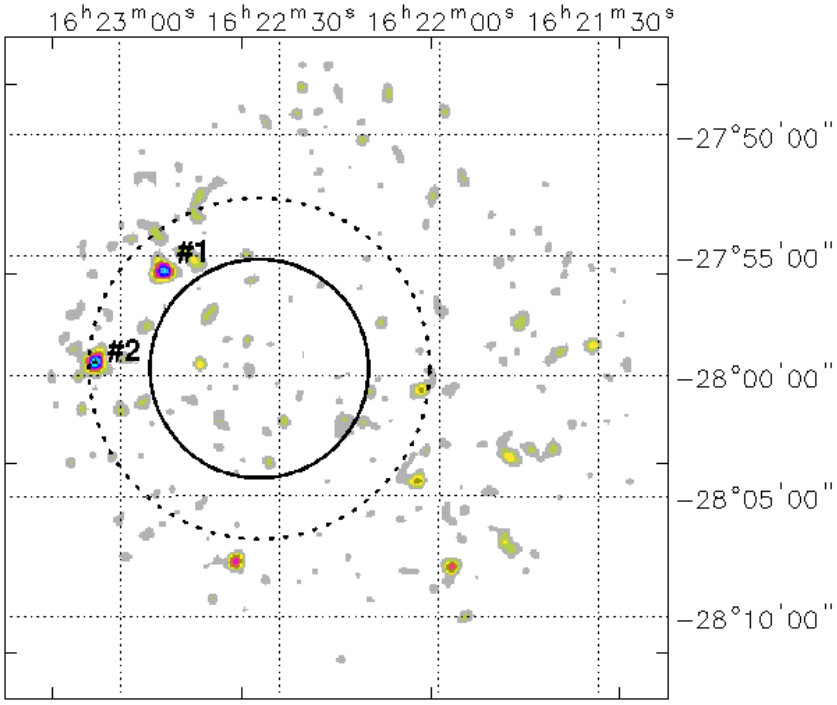

Figure 14: 0.3–10 keV XRT image of the IGR J16226–2759 field.

XRT detects two X–ray sources whose positions are compatible with the 99% IBIS positional uncertainty:

➢ Source #1, which lies inside the 90% IBIS error circle, is located at:

R.A.(J2000) = $16^{h}22^{m}51'.80$

Dec.(J2000) = $-27°55'37''.90$

error box = $6''.00$

It is detected at 4.7σ c.l. in the 0.3–10 keV energy band, and it is not visible above 3 keV.

Multi–wavelength counterparts to this XRT detection:

- USNO–A2.0 U0600.20352745 with magnitude $R = 14.3$, and $B = 16.2$;
- 2MASS J16225158–2755371 with magnitudes $J = 11.102 \pm 0.022$, $H = 10.463 \pm 0.022$, $K = 10.176 \pm 0.019$;
- WISE J162251.57–275537.3 with colours $W1 = 10.061 \pm 0.022$, $W2 = 9.909 \pm 0.020$, $W3 = 9.841 \pm 0.062$, and $W4 = 8.698 \pm 0.000$;
- 1SXPS J162252.1–275536;
- It is possibly a pre–main–sequence K/M star (Rizzuto et al. 2014).

➢ Source #2, which lies at the border of the 99% IBIS error circle, is located at:

R.A.(J2000) = $16^{\rm h}23^{\rm m}04'.60$

Dec.(J2000) = $-27^{\circ}59'25''.00$

error box = $6''.00$

It is detected at 5.1σ in the 0.3–10 keV energy range, but not above 3 keV.

Multi–wavelength counterparts to this XRT detection:

- USNO–A2.0 U0600.20361219 with magnitudes $R = 13.2$, and $B = 15.0$;
- 2MASS J16230474–2759252 with magnitudes $J = 10.516 \pm 0.022$, $H = 9.812 \pm 0.022$, $K = 9.555 \pm 0.021$;
- WISE J162304.73–275925.4 with colours $W1 = 9.498 \pm 0.023$, $W2 = 9.409 \pm 0.019$, $W3 = 9.254 \pm 0.037$, and $W4 = 8.657 \pm 0.000$;
- 1SXPS J162305.1–275921;
- It is possibly a pre–main–sequence K/M star (Rizzuto et al. 2014).

None of the two X–ray source seem to be a likely counterpart to this IBIS source, unless we are dealing with a peculiar type of object.

IGR J16327–4940

(IBIS detection: 0.9–day outburst)

One XRT observation available:

1. obscode: 00032483001
   observation date: 07/06/2012
   exposure: 2888 s

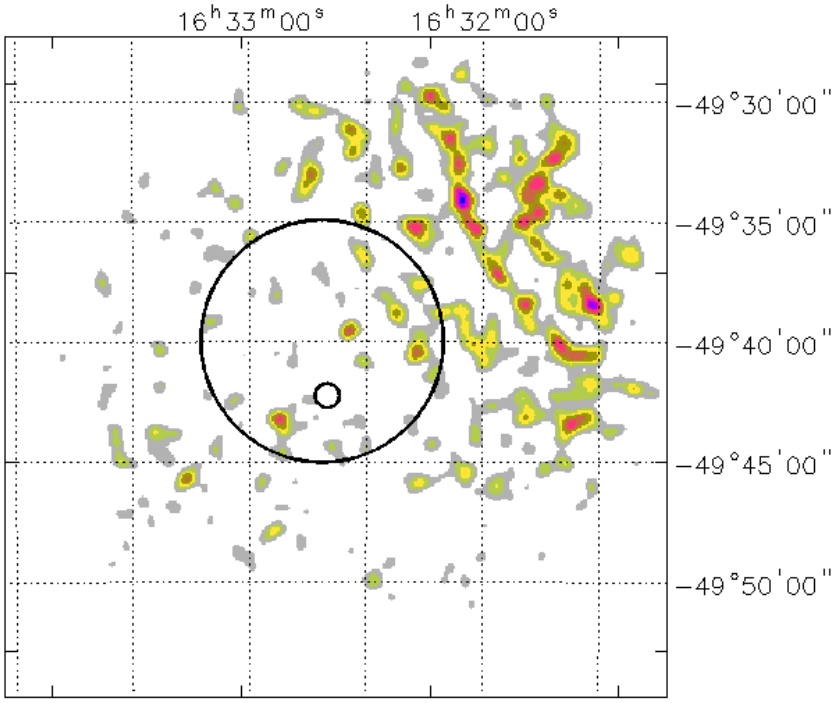

Figure 15: 0.3–10 keV XRT image of the IGR J16327+4940 field. The smaller black circle depicts the position of the counterpart to the IBIS object proposed by Masetti et al. (2010), which is not detected in X–rays.

No X–ray source has been found within the IBIS error circle.

This source was tentatively identified with VRMF 55 and classified by Masetti et al. (2010) as a HMXB (OB Giant) which is located within the IBIS positional uncertainty (see smaller black circle in Figure 15)

Unfortunately, the XRT observations available so far do not allow us to draw any firm conclusions about the nature of this high–energy source, but variability might be responsible for the observed discrepancy.

IGR J16388+3557

(IBIS detection: 0.6–day outburst)

One XRT observation available:

1. obscode: 00041221001
   observation date: 30/11/2010
   exposure: 3870 s

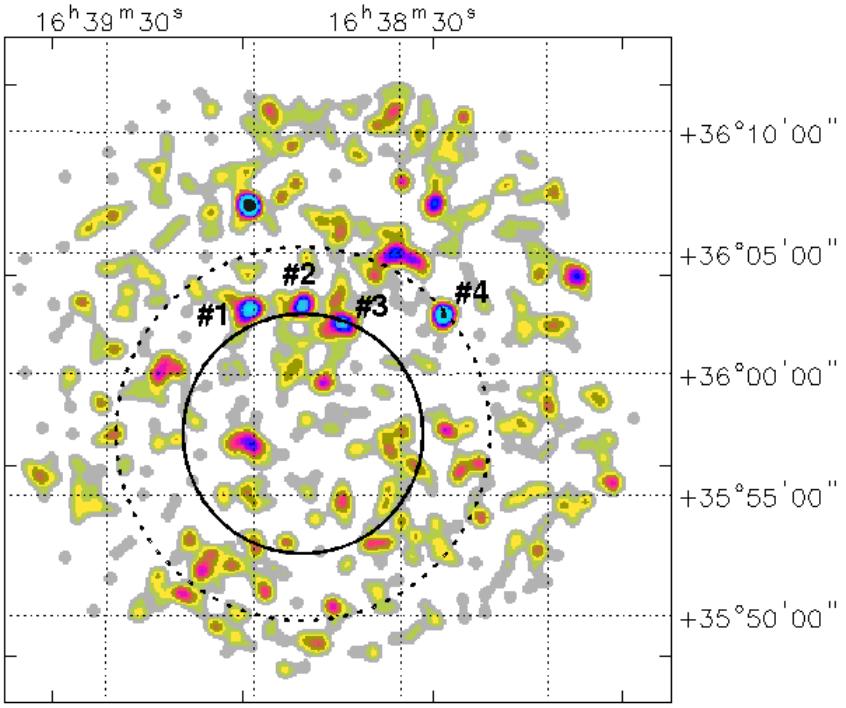

Figure 16: 0.3–10 keV XRT image of the IGR J16388+3557 field.

XRT detects four X–ray sources whose positions are compatible with either the 90% or the 99% IBIS positional uncertainties:

➢ Source #1, which lies just outside the 90% IBIS error circle, is located at:

R.A.(J2000) = $16^{h}39^{m}00'.50$

Dec.(J2000) = $+36^{\circ}02'43''.00$

error box = $6''.00$

It is detected at 2.8σ c.l. in the 0.3–10 keV energy band, and it is not visible above 3 keV.

Multi–wavelength counterparts to this XRT detection:

- 1SXPS J163900.9+360244.

➢ Source #2, which lies at the border of the 90% IBIS error circle, is located at:

R.A.(J2000) = $16^{\rm h}38^{\rm m}50'.10$

Dec.(J2000) = $+36^{\circ}02'48''.90$

error box = $6''.00$

It is detected at 2.9σ in the 0.3–10 keV energy range, but not above 3 keV.

Multi–wavelength counterparts to this XRT detection:

- WISE J163849.75+360243.7 with colours $W1 = 16.212 \pm 0.070$, $W2 = 15.146 \pm 0.089$, $W3 = 11.446 \pm 0.119$, and $W4 = 9.118 \pm 0.391$.

➢ Source #3, which lies at the border of the 90% IBIS error circle, is located at:

R.A.(J2000) = $16^{\rm h}38^{\rm m}41'.60$

Dec.(J2000) = $+36^{\circ}02'06''.60$

error box = $6''.00$

It is detected at 2.7σ c.l. in the 0.3–10 keV energy band, and it is not visible above 3 keV.

No counterpart has been found to this XRT detection.

➢ Source #4, which lies at the border of the 99% IBIS error circle, is located at:

R.A.(J2000) = $16^{\rm h}38^{\rm m}21'.10$

Dec.(J2000) = $+36^{\circ}02'29''.70$

error box = $6''.00$

It is detected at 3.2σ in the 0.3–10 keV energy range, but not above 3 keV.

Multi–wavelength counterparts to this XRT detection:

- USNO B–1.0 1260–0246237 with magnitudes $R2 = 21.00$, and $B2 = 20.74$;

- WISE J163821.23+360226.4 with colours $W1 = 16.757 \pm 0.105$, $W2 = 15.676 \pm 0.143$, $W3 = 12.385 \pm 0.286$, and $W4 = 9.354 \pm 0.000$;
- SDSS J163821.24+360226.4 a QSO candidate with $z = 0.445$;
- 1SXPS J163821.3+360228.

This source was classified by Masetti et al. (2012) as a Seyfert 1 at $z = 0.675$.

IGR J17468–2902

(IBIS detection: persistent)

One XRT observation available:

1. obscode: 00031926001
   observation date: 11/02/2011
   exposure: 7685 s

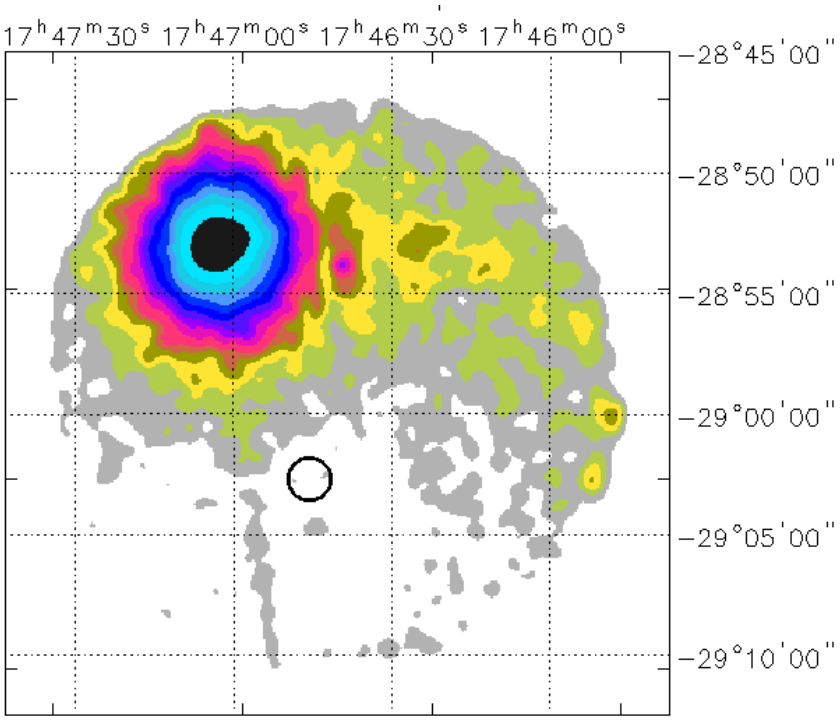

Figure 17: 0.3–10 keV XRT image of the IGR J17468–2902 field.

No X–ray source has been found within the 90% IBIS error circle. The bright source located at ∼10 arcminutes from the IBIS detection is the low mass X–ray binary KRL 2007b. A superburst from this source was observed on Feb 13, 2011 by JEM–X (Chenevez et al. 2011). On that occasion IBIS marginally detected the source.

IGR J17479–2807

(IBIS detection: persistent)

Thirty XRT observations available:

1. obscode: 00030938001
   observation date: 13/05/2007
   exposure: 4474 s

2. obscode: 00030938002
   observation date: 16/05/2007
   exposure: 1408 s

3. obscode: 00030938004
   observation date: 08/08/2007
   exposure: 1991 s

4. obscode: 00030938005
   observation date: 28/04/2008
   exposure: 2001 s

5. obscode: 00030938006
   observation date: 15/05/2009
   exposure: 1402 s

6. obscode: 00030938008
   observation date: 17/05/2010
   exposure: 3718 s

7. obscode: 00431582000
   observation date: 13/08/2010
   exposure: 2200 s

8. obscode: 00030938009
   observation date: 07/06/2011
   exposure: 667 s

9. obscode: 00030938011
   observation date: 23/06/2011
   exposure: 1988 s

10. obscode: 00030938012
    observation date: 06/05/2012
    exposure: 2114 s

11. obscode: 00032417001
    observation date: 13/05/2012
    exposure: 564 s

12. obscode: 00043660002
    observation date: 23/06/2012
    exposure: 524 s

13. obscode: 00032417002
    observation date: 06/09/2012
    exposure: 539 s

14. obscode: 00038003005
    observation date: 19/04/2013
    exposure: 176 s

15. obscode: 00038003006
    observation date: 21/04/2013
    exposure: 1632 s

16. obscode: 00038003007
    observation date: 05/05/2013
    exposure: 231 s

17. obscode: 00038003008
    observation date: 28/05/2013
    exposure: 163 s

18. obscode: 00038003009
    observation date: 03/06/2013
    exposure: 298 s

19. obscode: 00038003011
    observation date: 19/06/2013
    exposure: 1542 s

20. obscode: 00038003013
    observation date: 03/06/2013
    exposure: 298 s

21. obscode: 00030938013
    observation date: 01/03/2014
    exposure: 283 s

22. obscode: 00030938014
    observation date: 06/03/2014
    exposure: 411 s

23. obscode: 00030938015
    observation date: 09/03/2014
    exposure: 527 s

24. obscode: 00030938016
    observation date: 11/03/2014
    exposure: 130 s

25. obscode: 00030938017
    observation date: 20/03/2014
    exposure: 433 s

26. obscode: 00030938018
    observation date: 12/02/2015
    exposure: 93 s

27. obscode: 00030938019
    observation date: 17/02/2015
    exposure: 1989 s

28. obscode: 00030938021
    observation date: 17/03/2015
    exposure: 3257 s

29. obscode: 00030938022
    observation date: 13/04/2015
    exposure: 1941 s

30. obscode: 00030938023
    observation date: 13/05/2015
    exposure: 1843 s

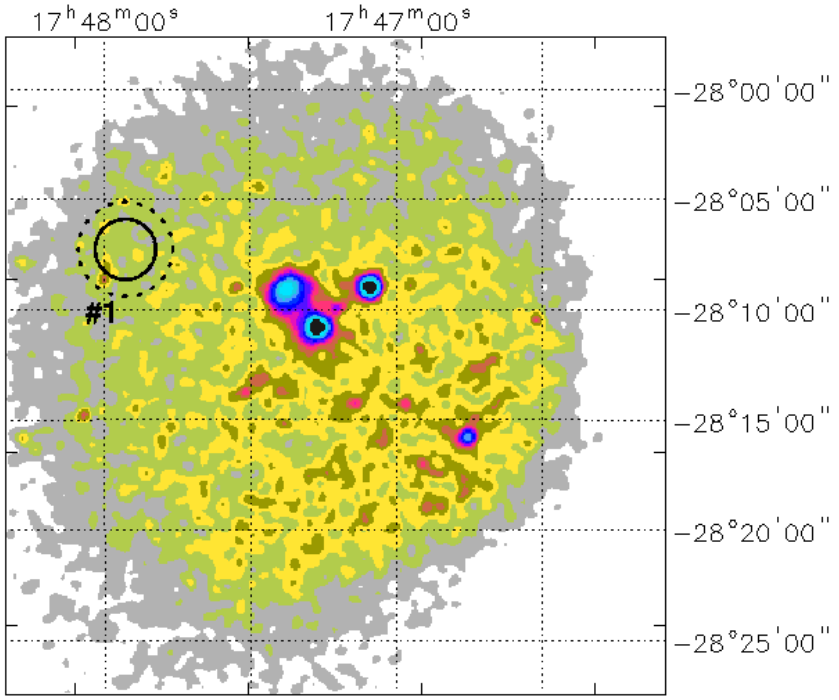

Figure 18: 0.3–10 keV XRT image of the IGRJ 174679–2807 field.

There is only one X–ray source detected by XRT inside the 99% IBIS positional uncertainty and it is located at:

R.A.(J2000) = $17^{\rm h}47^{\rm m}59'.90$

Dec.(J2000) = $-28^{\circ}08'37''.90$

error box = $6''.00$

It is detected at 3.7σ and 3.3σ c.l. in 0.3–10 keV energy band and above 3 keV, respectively.

Multi–wavelength counterparts to this XRT detection:

- USNO–A2.0 U0600.28802156 with magnitude $R = 17.5$, and $B = 20.8$;
- 2MASS J17475952–2808362 ($J = 14.574 \pm 0.047$, $H = 13.663 \pm 0.073$, and $K = 13.181 \pm 0.000$), and 2MASS J174800072808325 ($J = 15.661 \pm 0.000$, $H = 14.145 \pm 0.000$, and $K = 12.353 \pm 0.053$).

IGR J18175–1530

(IBIS detection: 35.3–day outburst)

One XRT observation available:

1. obscode: 00030991002
   observation date: 03/11/2011
   exposure: 1951 s

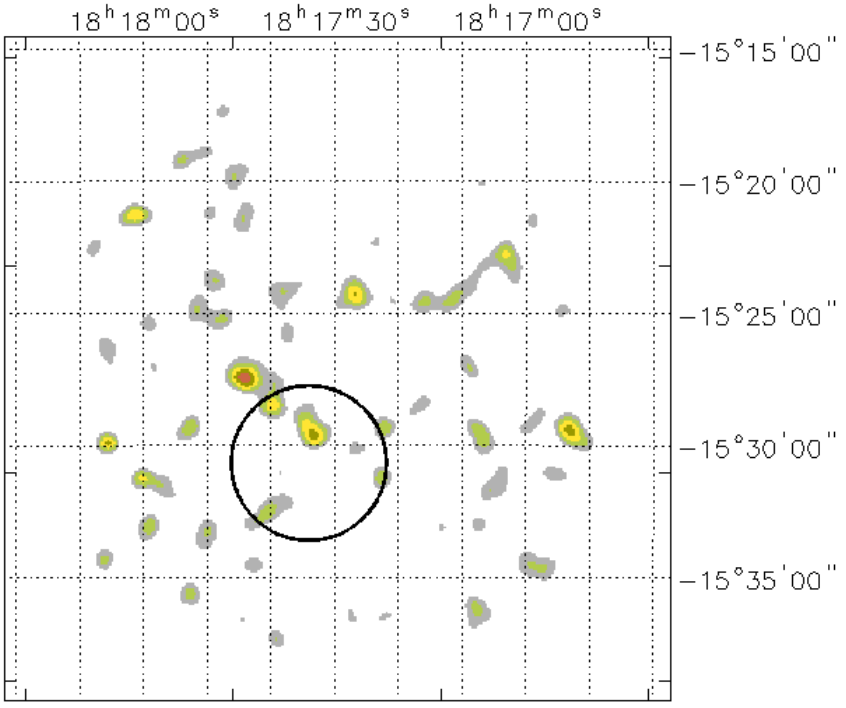

Figure 19: 0.3–10 keV XRT image of the IGRJ 18175–1530 field.

No X–ray source has been found within the IBIS error circle.

IGR J19079+0942

(IBIS detection: 0.5–day outburst)

One XRT observation available:

1. obscode: 00044828001
   observation date: 03/12/2011
   exposure: 499 s

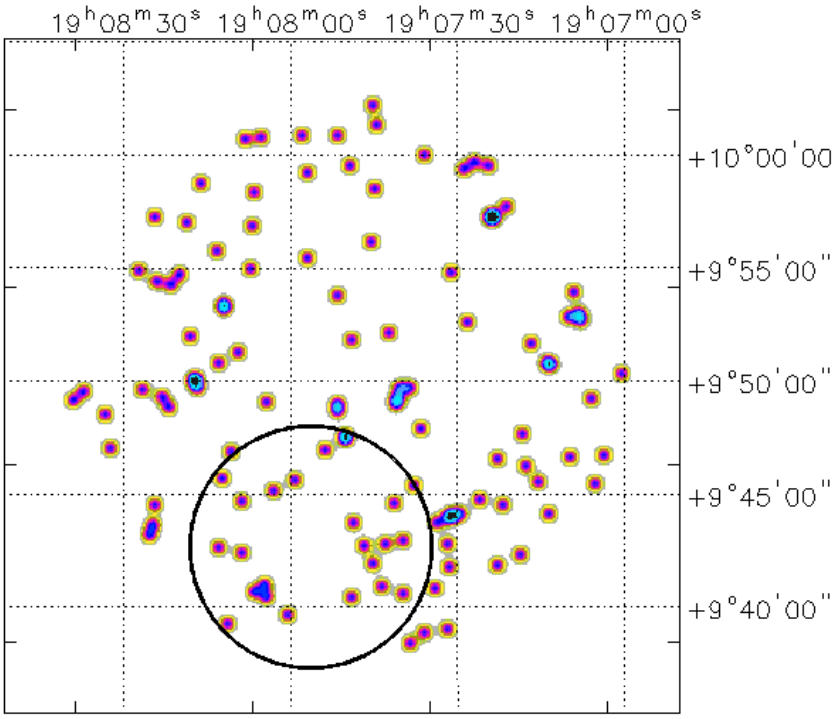

Figure 20: 0.3–10 keV XRT image of the IGR J19079+0942 field.

No X–ray source has been found within the IBIS error circle, maybe due to the low exposure.

IGR J19113+1533

(IBIS detection: 2.8–day outburst)

One XRT observation available:

1. obscode: 00041231001
   observation date: 26/05/2011
   exposure: 4763 s

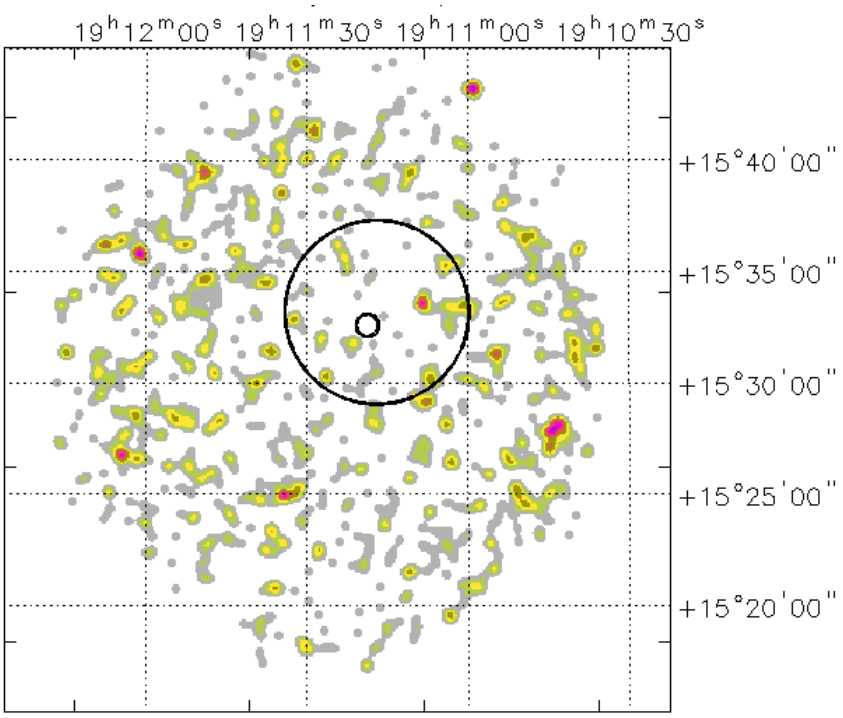

Figure 21: 0.3–10 keV XRT image of the IGR J19113+1533 field. The smaller black circle depicts the position of the putative counterpart proposed by Masetti et al. (2010).

No X–ray source has been found within the IBIS error circle.

The smaller black circle in Figure 21 depicts the putative optical counterpart (KW97 36–14) to the IBIS sources classified as a High Mass X–ray Binary (B[e]/X Binary ?) by Masetti et al. (2010). This source is not detected in X–rays by XRT, maybe because observed during a state of very low flux. Also in this case variability may play a key role.

IGR J19118+1125

(IBIS detection: 4.8–day outburst)

Two XRT observations available:

1. obscode: 00044877001
   observation date: 31/05/2012
   exposure: 316 s
2. obscode: 00044877002
   observation date: 12/06/2012
   exposure: 438 s

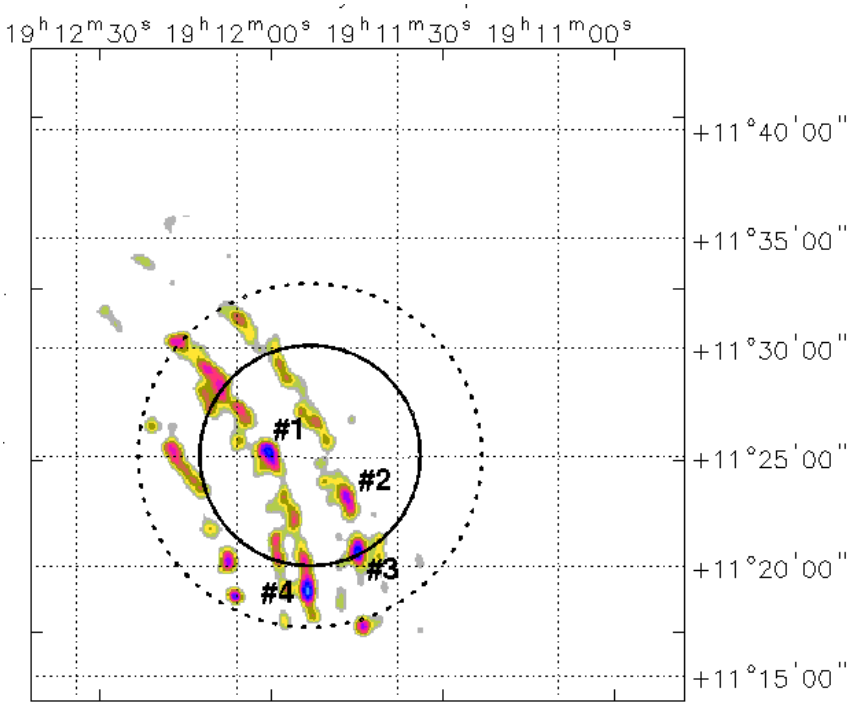

Figure 22: 0.3–10 keV XRT image of the IGRJ 19118+1125 field.

This case is unusual as structures in the XRT image are present altering the source detection method. For the sake of completeness, we report the positive detections we obtain, bearing in mind that they can be false detections.

Four possible X–ray objects have a position compatible with either the 90% or the 99% IBIS positional uncertainties:

➢ Source #1, which lies within the 90% IBIS error circle, is located at:

R.A.(J2000) = $19^h11^m54'.50$

Dec.(J2000) = $+11^{\circ}25'27''.30$

error box = $6''.00$

It is detected at 2.7σ c.l. in 0.3–10 keV energy band, and it is still visible above 3 keV at 3.0σ c.l.

Multi–wavelength counterparts to this XRT detection:

- UGPS J191154.59+112528.4 ($J = 18.868 \pm 0.110$, $H = 17.863 \pm 0.094$, and $K = 18.000 \pm 0.199$), UGPS J191154.34+112529.9 ($J = 16.578 \pm 0.014$, $H = 15.582 \pm 0.012$, and $K = 15.239 \pm 0.016$), UGPS J191154.26+112528.2 ($J = 16.143 \pm 0.010$, $H = 15.399 \pm 0.010$, and $K = 15.072 \pm 0.014$), UGPS J191154.66+112530.3 ($J = 18.304 \pm 0.066$, $H = 17.526 \pm 0.069$, and $K = 17.453 \pm 0.121$), UGPS J191154.60+112523.3 ($J = 0.000 \pm 0.000$, $H = 17.278 \pm 0.055$, and $K = 16.701 \pm 0.061$), UGPS J191154.27+112524.4 ($J = 19.002 \pm 0.124$, $H = 18.397 \pm 0.153$, and $K = 17.983 \pm 0.196$), and UGPS J191154.89+112527.5 ($J = 17.489 \pm 0.031$, $H = 16.783 \pm 0.035$, and $K = 16.604 \pm 0.055$).
- IPHAS2 J191154.29+112528.3 ($I = 18.53 \pm 0.04$), IPHAS2 J191154.34+112529.9 ($I = 19.53 \pm 0.10$), and IPHAS2 J191154.67+112530.3 ($I = 20.65 \pm 0.28$);
- G045.4158+00.7172 with magnitudes 3.6mag $= 14.249 \pm 0.147$, 4.5mag $= 14.508 \pm 0.299$, 5.8mag $= 0.000 \pm 0.000$, and 8mag $= 0.000 \pm 0.000$.

➢ Source #2, which lies within the 90% IBIS error circle, is located at:

R.A.(J2000) = $19^{\rm h}11^{\rm m}39'.20$

Dec.(J2000) = $+11^{\circ}23'16''.70$

error box = $6''.00$

It is detected at 3.0σ c.l. in 0.3–10 keV energy band, and is not revealed above 3 keV.

Multi–wavelength counterparts to this XRT detection:

- USNO–B1.0 1013–0443527 with magnitude $B2 = 19.95$;
- 2MASS J19113926+1123185 ($J = 15.406 \pm 0.090$, $H = 14.078 \pm 0.069$, and $K = 13.376 \pm 0.000$), and 2MASS J19113943+1123161 ($J = 15.463 \pm 0.082$, $H = 14.525 \pm 0.070$, and $K = 13.369 \pm 0.000$).

➢ Source #3, which lies at the border of the 90% IBIS error circle, is located at:

R.A.(J2000) = $19^{\rm h}11^{\rm m}37'.30$

Dec.(J2000) = $+11^{\circ}20'53''.90$

error box = $6''.00$

This source is detected at 2.6σ c.l. in 0.3–10 keV; no detection is found above 3 keV.

Multi–wavelength counterparts to this XRT detection:

- USNO–A2.0 U0975.14312019 with magnitudes $R = 15.5$, and $B = 17.4$;
- 2MASS J19113749+1120517 with magnitudes $J = 13.672 \pm 0.053$, $H = 13.201 \pm 0.060$, and $K = 12.952 \pm 0.094$.

➢ Source #4, which lies within the 99% IBIS error circle, is located at:

R.A.(J2000) = $19^{\rm h}11^{\rm m}46'.60$

Dec.(J2000) = $+11^{\circ}18'51''.90$

error box = $6''.00$

This source is detected at 3.2σ c.l. in both the 0.3–10 keV energy range and above 3 keV.

Multi–wavelength counterparts to this XRT detection:

- 2MASS J19114687+1118529 with magnitudes $J = 15.827 \pm 0.083$, $H = 15.005 \pm 0.000$, and $K = 14.451 \pm 0.000$.

By extracting the XRT image in the 3–10 keV energy band, we note that, apart from source #1 and #4 discussed above, there are two other sources detected by XRT (see Figure 23):

➢ Source #5, which lies within the 90% IBIS error circle, is located at:

R.A.(J2000) = $19^{\rm h}11^{\rm m}52'.00$

Dec.(J2000) = $+11^{\circ}29'26''.80$

error box = $6''.00$

It is detected at 2.5σ c.l. in 3–10 keV energy band.

Multi–wavelength counterparts to this XRT detection:

- UGPS J191152.02+112927.0 ($J = 18.411 \pm 0.072$, $H = 17.605 \pm 0.074$, and $K = 17.256 \pm 0.100$), UGPS J191152.12+112924.3 ($J = 18.916 \pm 0.114$, $H = 17.613 \pm 0.074$, and $K = 17.253 \pm 0.100$), UGPS J191152.21+112926.6 ($J = 18.580 \pm 0.084$, $H = 17.826 \pm 0.090$, and $K = 17.407 \pm 0.115$), UGPS J191152.21+112928.4 ($J = 20.223 \pm 0.379$, $H = 18.978 \pm$

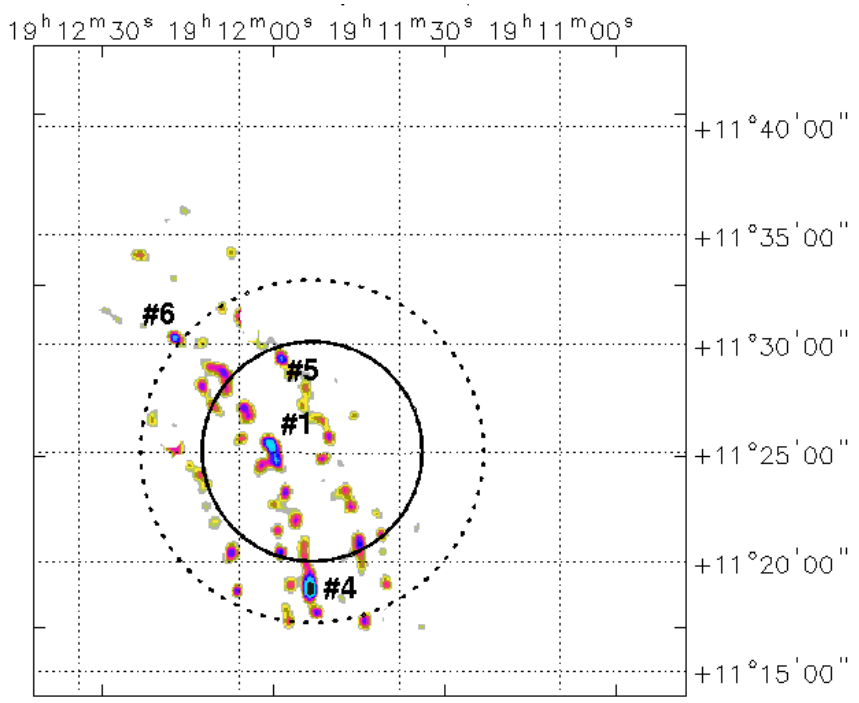

Figure 23: 3–10 keV XRT image of the IGRJ19118+1125 field.

0.260, and $K = 18.514 \pm 0.318$), UGPS J191151.73+112926.4 ($J = 18.061 \pm 0.052$, $H = 17.342 \pm 0.058$, and $K = 16.768 \pm 0.064$), UGPS J191151.78+112930.2 ($J = 18.509 \pm 0.079$, $H = 17.391 \pm 0.061$, and $K = 17.012 \pm 0.080$), UGPS J191151.85+112931.1 ($J = 0.000 \pm 0.000$, $H = 17.875 \pm 0.094$, and $K = 17.295 \pm 0.104$), UGPS J191151.82+112921.7 ($J = 19.072 \pm 0.132$, $H = 18.306 \pm 0.140$, and $K = 17.891 \pm 0.179$), and UGPS J191151.93+112932.6 ($J = 0.000 \pm 0.000$, $H = 19.139 \pm 0.302$, and $K = 19.745 \pm 0.986$).

➢ Source #6, which lies within the 90% IBIS error circle, is located at:

R.A.(J2000) = $19^{h}12^{m}12'.00$

Dec.(J2000) = $+11^{\circ}30'17''.70$

error box = $6''.00$

It is detected at 2.3σ c.l. in 3–10 keV energy band.

Multi–wavelength counterparts to this XRT detection:

- G045.5218+00.6900 with magnitudes 3.6mag $= 14.683 \pm 0.183$, 4.5mag $= 14.002 \pm 0.227$, 5.8mag $= 0.000 \pm 0.000$, and 8mag $= 0.000 \pm 0.000$;
- several sources listed in the UKIDSS–DR6 Galactic Plane Survey.

As a conclusion, we stress the fact that it is likely that all these detections are simply artifacts in the X–ray image and not real sources.

IGR J19294–1746

(IBIS detection: 0.5–day outburst)

Five XRT observations available:

1. obscode: 00084533001
   observation date: 29/07/2014
   exposure: 604 s
2. obscode: 00084533002
   observation date: 01/08/2014
   exposure: 1088 s
3. obscode: 00084533003
   observation date: 05/08/2014
   exposure: 741 s
4. obscode: 00084533004
   observation date: 12/08/2014
   exposure: 469 s
5. obscode: 00084533005
   observation date: 14/08/2014
   exposure: 863 s

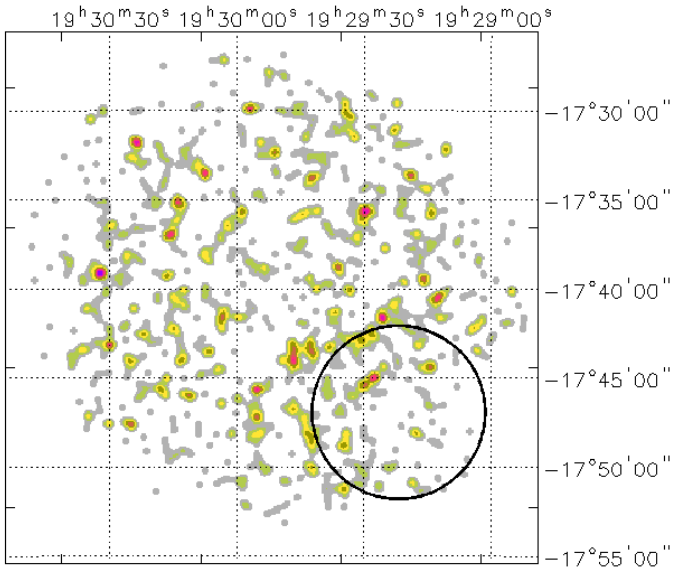

Figure 24: 0.3–10 keV XRT image of the IGR J19294–1746 field.

No X–ray source has been found within the IBIS error circle.

IGR J19295–0919

(IBIS detection: 14.2–day outburst)

One XRT observation available:

1. obscode: 00041234001
   observation date: 27/11/2010
   exposure: 5167 s

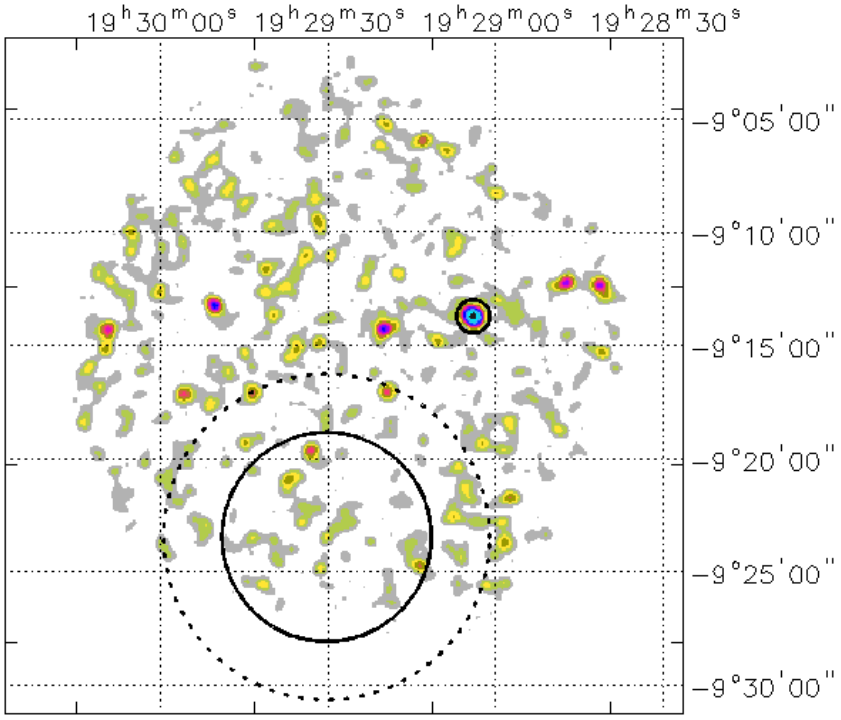

Figure 25: 0.3–10 keV XRT image of the IGR J19295–0919 field. The smaller black circle depicts the position of the counterpart proposed by Masetti et al. (2013).

No X–ray source has been found within the IBIS error circle.

The smaller black circle in Figure 25 represents the counterpart to the IBIS source proposed by Masetti et al. (2013) and classified as a type 2 QSO at $z = 0.741$. This X–ray source is located around 4.5 arcmin from the border of the 99% IBIS positional uncertainty, which makes it an unlikely association with the high–energy emitter.

IGR J21268+6203

(IBIS detection: 2.4–day outburst)

Six XRT observations available:

1. obscode: 00045405001
   observation date: 05/04/2011
   exposure: 868 s

2. obscode: 00045405002
   observation date: 08/04/2011
   exposure: 777 s

3. obscode: 00045405003
   observation date: 24/06/2011
   exposure: 1587 s

4. obscode: 00045405004
   observation date: 09/07/2011
   exposure: 498 s

5. obscode: 00045405005
   observation date: 16/07/2011
   exposure: 1758 s

6. obscode: 00045405006
   observation date: 17/07/2011
   exposure: 5386 s

Maiorano et al. (2011), based on the cross–correlation of the list of unidentified IBIS sources listed in the fourth catalogue first with infrared and then radio catalogues, proposed 2MASX J21262644+6204410 as a good candidate for an association with the IBIS source. Unfortunately, this source (smaller black circle in Figure 26) is not detected in X–rays, casting doubts on its associations with the IBIS source. However, other objects are found to emit X–ray within the IBIS positional uncertainty and these are discussed in the following.

XRT detects six X–ray objects whose position is compatible either with the 90% or the 99% IBIS error circles:

➢ Source #1, which lies within the 90% IBIS error circle, is located at:

R.A.(J2000) = $21^{h}26^{m}54'.50$

Dec.(J2000) = $+62^{\circ}05'08''.20$

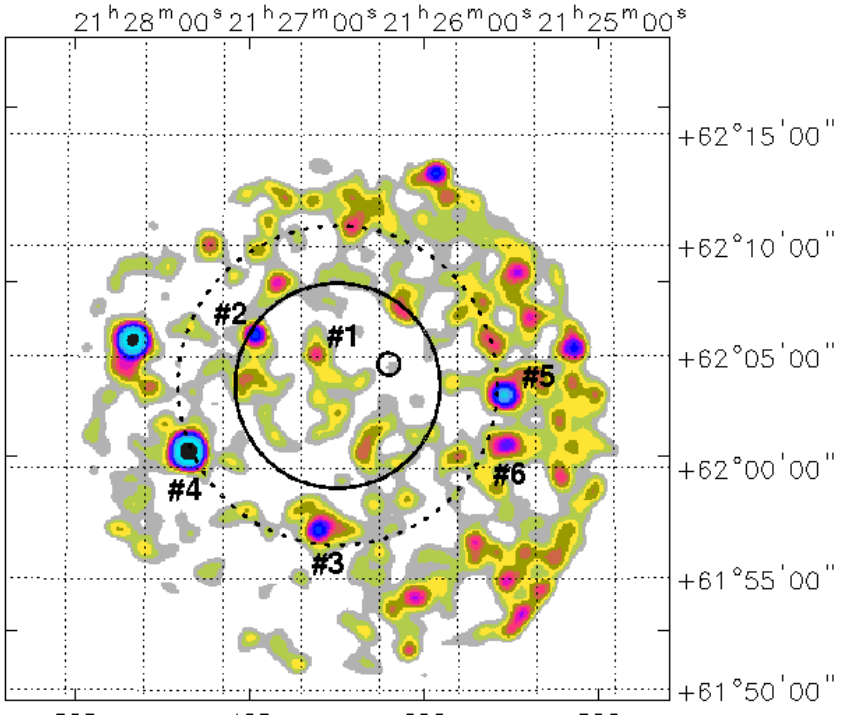

Figure 26: 0.3–10 keV XRT image of the IGR J21268+6203 field. The small black circle depicts the position of 2MASX J21262644+6204410, proposed by Maiorano et al. (2011) as a good candidate for an association with the IBIS source.

error box = $6''.00$

It is detected at 2.7σ c.l. in 0.3–10 keV energy band, and it is not visible above 3 keV.

No counterpart has been found to this XRT detection.

From the X–ray data we can only infer a 2–10 keV flux of $\sim 4 \times 10^{-14}$ erg cm^{-2} s^{-1} by assuming a power law continuum (photon index frozen to 1.8) passing through the Galactic absorption ($N_{\rm H(Gal)} = 2.97 \times 10^{21}$ cm^{-2}).

➢ Source #2, which is detected at the border of the 90% IBIS error circle, is located at:

R.A.(J2000) = $21^{\rm h}27^{\rm m}17'.60$

Dec.(J2000) = $+62°06'02''.20$

error box = $6''.00$

It is detected at 4.2σ c.l. in 0.3–10 keV energy band, and is not revealed above 3 keV.

Multi–wavelength counterparts to this XRT detection:

- USNO–A2.0 U1500.08051773 with magnitudes $R = 10.9$, and $B = 8.6$;
- 2MASS J21271790+6206035 with magnitudes $J = 4.965 \pm 0.037$, $H = 4.486 \pm 0.015$, and $K = 4.320 \pm 0.051$;
- WISE J212717.86+620603.7 with colours $W1 = 4.218 \pm 0.095$, $W2 = 3.763 \pm 0.057$, $W3 = 4.218 \pm 0.014$, and $W4 = 4.149 \pm 0.024$;
- 1SXPS J212717.6+620602;
- Star HD 204612 of spectral type K0 D.

Because of the poor statistical quality of the X–ray data, we can only infer a 2–10 keV flux of $\sim 1 \times 10^{-14}$ erg cm^{-2} s^{-1} by assuming a bremsstrahlung component ($kT \sim 0.5$ keV) passing through the Galactic absorption ($N_{\rm H(Gal)} = 2.99 \times 10^{21}$ cm^{-2}).

➢ Source #3, which lies within the 99% IBIS error circle, is located at:

R.A.(J2000) = $21^{\rm h}26^{\rm m}53'.40$

Dec.(J2000) = $+61^{\circ}57'14''.20$

error box = $6''.00$

This source is detected at 4.3σ c.l. in 0.3–10 keV, and it is still visible above 3 keV at 2.3σ c.l.

Multi–wavelength counterparts to this XRT detection:

- WISE J212653.69+615715.9 with colours $W1 = 15.339 \pm 0.045$, $W2 = 14.401 \pm 0.040$, $W3 = 11.625 \pm 0.090$, and $W4 = 9.513 \pm 0.000$;
- 1SXPS J212653.5+615713.

From the X–ray data we can only infer a 2–10 keV flux of $\sim 8 \times 10^{-14}$ erg cm^{-2} s^{-1} by assuming a power law continuum (photon index frozen to 1.8) passing through the Galactic absorption ($N_{\rm H(Gal)} = 2.99 \times 10^{21}$ cm^{-2}).

➢ Source #4 lies at the border of the 99% IBIS error circle and it is located at:

R.A.(J2000) = $21^{\rm h}27^{\rm m}43'.10$

Dec.(J2000) = $+62^{\circ}00'46''.10$

error box = $6''.00$

It is detected at 10.8σ c.l. in 0.3–10 keV energy band; no detection is found above 3 keV.

Multi–wavelength counterparts to this XRT detection:

- USNO–A2.0 U1500.08057632 with magnitudes $R = 11.2$, and $B = 12.6$;
- 2MASS J21274305+6200458 with magnitudes $J = 9.424 \pm 0.027$, $H = 9.008 \pm 0.031$, and $K = 8.900 \pm 0.021$;
- WISE J212743.13+620046.2 with colours $W1 = 8.795 \pm 0.022$, $W2 = 8.824 \pm 0.020$, $W3 = 8.676 \pm 0.019$, and $W4 = 8.134 \pm 0.112$;
- 1SXPS J212743.0+620044;
- *ROSAT* Faint source 1RXS J212743.8+620048;
- Star TYC 4253–1558–1. The source spectral type if rK0 V as reported by Pickles & De Pagne (2010).

For this object we can estimate a 2–10 keV flux of $\sim 3 \times 10^{-14}$ erg cm^{-2} s^{-1} by assuming a bremsstrahlung component ($kT \sim 0.5$ keV) passing through the Galactic absorption ($N_{\rm H(Gal)} = 3.03 \times 10^{21}$ cm^{-2}).

➢ Source #5, which lies at the border of the 99% IBIS error circle, is located at:

R.A.(J2000) = $21^{\rm h}25^{\rm m}42'.00$

Dec.(J2000) = $+62^{\circ}03'18''.70$

error box = $6''.00$

It is detected at 5.0σ c.l. in 0.3–10 keV energy band, but it is not observed above 3 keV.

Multi–wavelength counterparts to this XRT detection:

- USNO–B1.0 1520–0331366 with magnitudes $R1 = 19.18$, and $R2 = 19.48$;
- WISE J212542.01+620317.4 with colours $W1 = 14.174 \pm 0.027$, $W2 = 13.475 \pm 0.038$, $W3 = 12.495 \pm 0.372$, and $W4 = 8.972 \pm 0.000$;
- 1SXPS J212542.0+620316.

A simple power law passing through Galactic absorption ($N_{\rm H(Gal)} = 2.91 \times 10^{21}$ cm^{-2}) provides a photon index $\Gamma = \left(1.04^{+0.59}_{-0.57}\right)$ and a 2–10 keV flux around 4×10^{-13} erg cm^{-2} s^{-1}.

➢ Source #6, which lies at the border of the 99% IBIS error circle, is located at:

R.A.(J2000) = $21^{\rm h}25^{\rm m}40'.10$

Dec. (J2000) = $+62^{\circ}01'04''.10$

error box = $6''.00$

It is detected at 2.9σ c.l. in 0.3–10 keV energy band, and it is not visible above 3 keV.

Multi–wavelength counterparts to this XRT detection:

- USNO–B1.0 1520–0331351 with magnitudes $R1 = 18.38$, $R2 = 18.25$, and $B2 = 20.26$;
- 2MASS J21254058+6201071 with magnitudes $J = 15.825 \pm 0.085$, $H = 15.062 \pm 0.094$, and $K = 14.955 \pm 0.135$;
- AllWISE J212540.61+620108.6 with colours $W1 = 14.752 \pm 0.042$, $W2 = 14.756 \pm 0.080$, $W3 = 12.555 \pm 0.000$, and $W4 = 8.622 \pm 0.000$;
- 1SXPS J212540.8+620105.

From the X–ray data we can only infer a 2–10 keV flux of $\sim 3 \times 10^{-14}$ erg cm^{-2} s^{-1} by assuming a power law continuum (photon index frozen to 1.8) passing through the Galactic absorption ($N_{\mathrm{H(Gal)}} = 2.91 \times 10^{21}$ cm^{-2}).

IGR J21319+3619

(IBIS detection: 36.7–day outburst)

Two XRT observations available:

1. obscode: 00041240001
   observation date: 17/02/2011
   exposure: 3831 s

2. obscode: 00041240002
   observation date: 20/02/2011
   exposure: 5007 s

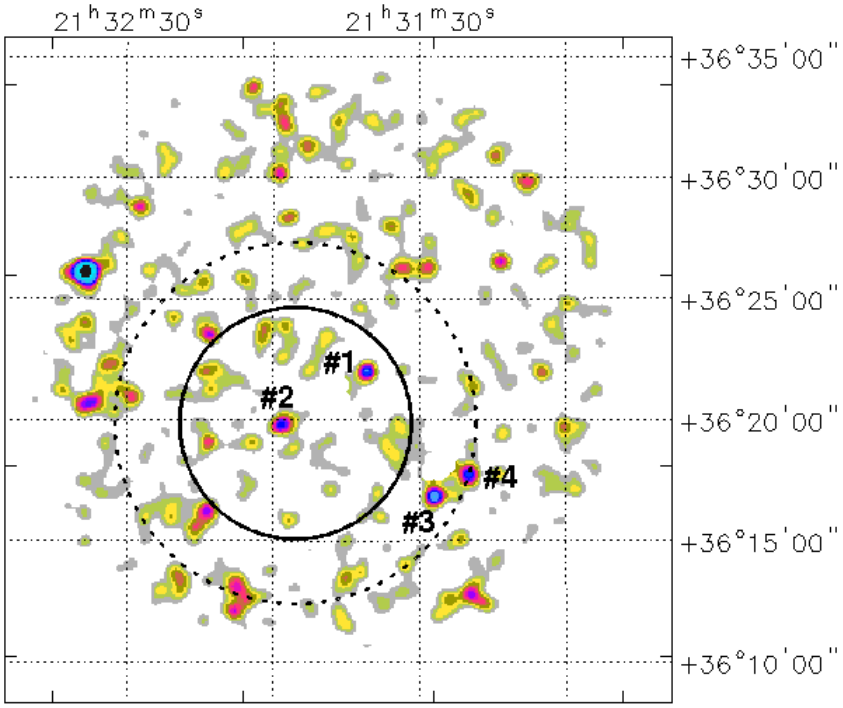

Figure 27: 0.3–10 keV XRT image of the IGR J21319+3619 field.

XRT detects four X–ray objects whose positions are compatible with either the 90% or 99% IBIS positional uncertainties::

➢ Source #1 lies within the 90% IBIS error circle and it is located at:

R.A.(J2000) = $21^h31^m40'.60$

Dec.(J2000) = $+36°21'58''.70$

error box = $6''.00$

It is detected at 2.8σ c.l. in 0.3–10 keV energy band, and it is not visible above 3 keV.

Multi–wavelength counterparts to this XRT detection:

- WISE J213140.69+362153.3 with colours $W1 = 15.185 \pm 0.040$, $W2 = 14.807 \pm 0.069$, $W3 = 12.785 \pm 0.519$, and $W4 = 9.055 \pm 0.000$;
- 1SXPS J213140.6+362157.

➢ Source #2, which is detected within the 90% IBIS error circle, is located at:

R.A.(J2000) = $21^{\rm h}31^{\rm m}58'.30$

Dec.(J2000) = $+36^\circ 19'48''.50$

error box = $6''.00$

It is detected at 2.6σ c.l. in 0.3–10 keV energy band, and is not revealed above 3 keV.

Multi–wavelength counterparts to this XRT detection:

- USNO–A2.0 U1200.18116486 with magnitudes $R = 18.5$, and $B = 19.9$;
- AllWISE J213158.11+361944.5 with colours $W1 = 16.444 \pm 0.070$, $W2 = 15.732 \pm 0.113$, $W3 = 12.400 \pm 0.000$, and $W4 = 9.154 \pm 0.000$;
- 1SXPS J213158.1+361951.

➢ Source #3, which lies within the 99% IBIS error circle, is located at:

R.A.(J2000) = $21^{\rm h}31^{\rm m}26'.70$

Dec.(J2000) = $+36^\circ 16'50''.50$

error box = $6''.00$

This source is detected at 3.1σ c.l. in 0.3–10 keV; no detection is found above 3 keV.

Multi–wavelength counterparts to this XRT detection:

- 1SXPS J213126.8+361649.

This source has been proposed as the counterpart to IGR J21319+3619 by Masetti et al. (2013) and classified as a type 1 QSO at $z = 1.488$.

➢ Source #4, which lies at the border of the 99% IBIS error circle, is located at:

R.A.(J2000) = $21^{\rm h}31^{\rm m}19'.80$

Dec.(J2000) = $+36^{\circ}17'48''.10$

error box = $6''.00$

This source is detected at 2.7σ c.l. in 0.3–10 keV; no detection is found above 3 keV.

No counterpart has been found to this XRT detection.

IGR J22014+6034

(IBIS detection: persistent)

Two XRT observations available:

1. obscode: 00041242001
   observation date: 11/07/2010
   exposure: 3725 s
2. obscode: 00041242002
   observation date: 14/07/2010
   exposure: 6066 s

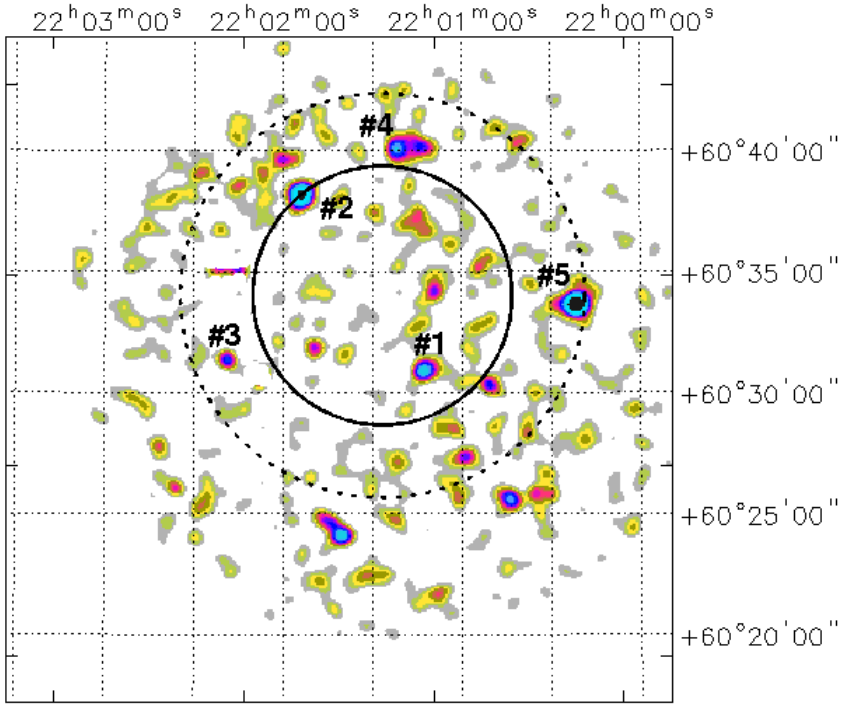

Figure 28: 0.3–10 keV XRT image of the IGR J22014+6034 field.

XRT detects five X–ray objects whose position are compatible with either the 90% or the 99% IBIS positional uncertainties:

➢ Source #1 lies within the 90% IBIS error circle and it is located at:

R.A.(J2000) = $22^{h}01^{m}12'.90$

Dec.(J2000) = $+60^{\circ}30'54''.00$

error box = $6''.00$

It is detected at 2.8σ c.l. in 0.3–10 keV energy band, but it is not visible above 3 keV.

Multi–wavelength counterparts to this XRT detection:

- 1SXPS J220113.1+603054.

➢ Source #2, detected at the border of the 90% IBIS error circle, is located at:

R.A.(J2000) = $22^{\rm h}01^{\rm m}53'.80$

Dec.(J2000) = $+60^\circ38'12''.20$

error box = $6''.00$

It is detected at 4.7σ c.l. in 0.3–10 keV energy band, and is not revealed above 3 keV.

Multi–wavelength counterparts to this XRT detection:

- USNO–B1.0 1506–0321399 ($B1 = 14.08$, and $B2 = 14.14$) and USNO–B1.0 1506-0321404 ($R1 = 11.77$, $R2 = 12.46$, and $B1 = 14.59$);
- 2MASS J22015416+6038094 with magnitudes $J = 11.504 \pm 0.025$, $H = 11.114 \pm 0.032$, and $K = 10.941 \pm 0.020$;
- WISE J220154.11+603809.5 with colours $W1 = 10.679 \pm 0.022$, $W2 = 10.728 \pm 0.021$, $W3 = 11.021 \pm 0.110$, and $W4 = 9.535 \pm 0.000$;
- Star CXOU J220154.1+603809;
- 1SXPS J220153.9+603811.

➢ Source #3, detected within the 99% IBIS error circle, is located at:

R.A.(J2000) = $22^{\rm h}02^{\rm m}18'.80$

Dec.(J2000) = $+60^\circ31'21''.90$

error box = $6''.00$

This source is detected at 2.6σ c.l. in 0.3–10 keV; no detection is found above 3 keV.

Multi–wavelength counterparts to this XRT detection:

- USNO–B1.0 1505–0323048 with magnitudes $R1 = 18.30$, $R2 = 18.57$, $B1 = 19.63$, and $B2 = 19.78$;

- 2MASS J22021926+6031268 with magnitudes $J = 16.477 \pm 0.148$, $H = 16.025 \pm 0.308$, and $K = 15.517 \pm 0.213$;
- WISE J220217.97+603118.8 with colours $W1 = 14.382 \pm 0.032$, $W2 = 14.222 \pm 0.048$, $W3 = 11.986 \pm 0.000$, and $W4 = 9.244 \pm 0.000$ (6.8 arcseconds away from the XRT centroid);
- 1SXPS J220218.0+603120.

➢ Source #4, detected within the 99% IBIS error circle, is located at:

R.A.(J2000) = $22^{\rm h}01^{\rm m}21'.70$

Dec.(J2000) = $+60^\circ 40' 08''.30$

error box = $6''.00$

This source is detected at 2.6σ c.l. in 0.3–10 keV; no detection is found above 3 keV.

Multi–wavelength counterparts to this XRT detection:

- USNO–B1.0 1506–0321050 with magnitudes $R2 = 18.89$, and $B2 = 20.34$;
- 2MASS J22012118+6040062 with magnitudes $J = 16.597 \pm 0.156$, $H = 15.870 \pm 0.169$, and $K = 15.496 \pm 0.203$;
- WISE J220121.31+604006.3 with colours $W1 = 15.735 \pm 0.059$, $W2 = 16.450 \pm 0.326$, $W3 = 11.665 \pm 0.142$, and $W4 = 9.351 \pm 0.393$;
- 1SXPS J220121.7+604006.

➢ Source #5, detected within the 99% IBIS error circle, is located at:

R.A.(J2000) = $22^{\rm h}00^{\rm m}21'.40$

Dec.(J2000) = $+60^\circ 33' 38''.70$

error box = $6''.00$

This source is detected at 5.4σ c.l. in 0.3–10 keV; no detection is found above 3 keV.

Multi–wavelength counterparts to this XRT detection:

- USNO–A2.0 U1500.08655368 with magnitudes $R = 13.7$, and $B = 15.5$;
- 2MASS J22002116+6033420 with magnitudes $J = 11.661 \pm 0.029$, $H = 10.989 \pm 0.033$, and $K = 10.817 \pm 0.020$;
- WISE J220021.22+603342.1 with colours $W1 = 10.710 \pm 0.023$, $W2 = 10.713 \pm 0.020$, $W3 = 10.274 \pm 0.044$, and $W4 = 8.453 \pm 0.175$ (6.8 arcseconds away from the XRT centroid);

- Star CXOU J220021.1+603342;
- 1SXPS J220021.2+603342.

The X–ray spectrum is modelled with a bremsstrahlung component ($N_{\mathrm{H(Gal)}} = 6.35 \times 10^{21}$ cm^{-2}) with $kT \sim 0.2$ keV and a 2–10 keV flux of $\sim 1 \times 10^{-15}$ erg cm^{-2} s^{-1}.

IGR J22253+5046

(IBIS detection: 5.9–day outburst)

One XRT observation available:

1. obscode: 00041243001
   observation date: 12/07/2011
   exposure: 5019 s

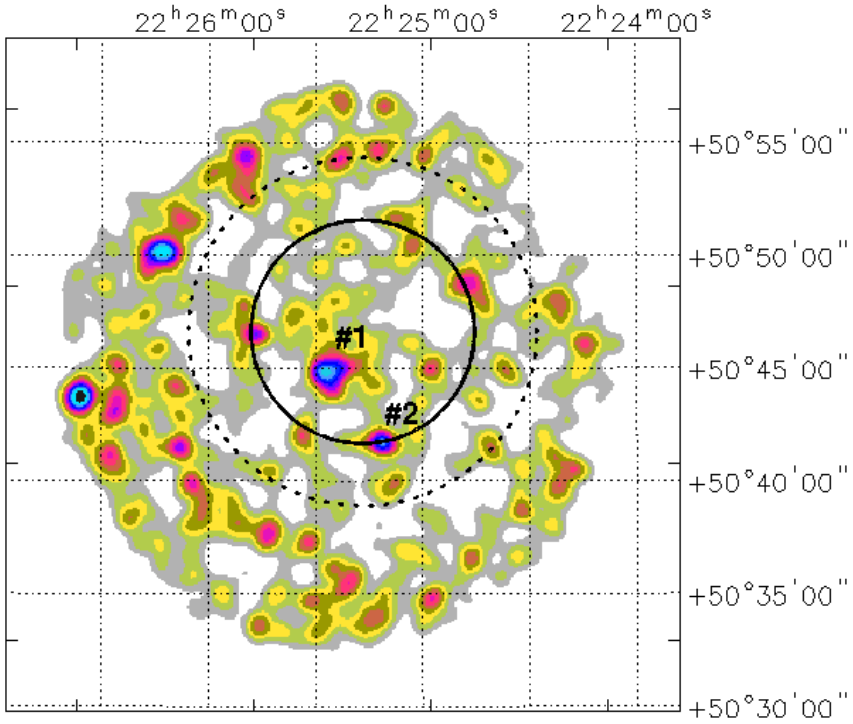

Figure 29: 0.3–10 keV XRT image of the IGR J22253+5046 field.

XRT detects two X–ray objects whose position are compatible with the 90% IBIS positional uncertainty:

➢ Source #1 lies within the 90% IBIS error circle and it is located at:

R.A.(J2000) = $22^h25^m28'.30$

Dec.(J2000) = $+50°44'54''.30$

error box = $6''.00$

It is detected at 2.5σ c.l. in 0.3–10 keV energy band, and it is not visible above 3 keV.

Multi–wavelength counterparts to this XRT detection:

- USNO–A2.0 U1350.16590129 with magnitudes $R = 11.6$, and $B = 12.3$;
- 2MASS J22252865+5044494 with magnitudes $J = 10.339 \pm 0.026$, $H = 10.132 \pm 0.030$, and $K = 10.076 \pm 0.019$;
- WISE J222528.67+504449.4 with colours $W1 = 10.026 \pm 0.023$, $W2 = 10.058 \pm 0.021$, $W3 = 9.937 \pm 0.036$, and $W4 = 8.879 \pm 0.289$;
- 1SXPS J222528.3+504447;
- Star BD+50 3709s and star TYC 3619–3890–1 of spectral type F2 D and F8 D, respectively. Note also that various stars fall within the XRT positional uncertainty.

The X–ray spectrum is modelled with a bremsstrahlung component ($N_{\rm H(Gal)} = 2.71 \times 10^{21}$ cm^{-2}) with $kT \sim 0.3$ keV and a 2–10 keV flux of $\sim 6 \times 10^{-15}$ erg cm^{-2} s^{-1}.

➢ Source #2 lies at the border of the 90% IBIS error circle and it is located at:

R.A.(J2000) = $22^{\rm h}25^{\rm m}11'.20$

Dec.(J2000) = $+50^{\circ}41'45''.10$

error box = $6''.00$

It is detected at 2.6σ c.l. in 0.3–10 keV energy band, and is not revealed above 3 keV.

Multi–wavelength counterparts to this XRT detection:

- USNO–A2.0 U0150.05103866 with magnitudes $R = 15.2$, and $B = 15.4$;
- 2MASS J22251151+5041483 with magnitudes $J = 12.442 \pm 0.034$, $H = 11.983 \pm 0.037$, and $K = 11.838 \pm 0.028$;
- WISE J222511.51+504148.6 with colours $W1 = 11.643 \pm 0.022$, $W2 = 11.706 \pm 0.023$, $W3 = 11.863 \pm 0.170$, and $W4 = 8.881 \pm 0.000$;
- *ROSAT* Faint source 1RXS J222512.5+504149 (14 arcseconds error radius);
- 1SXPS J222511.1+504144.

Given the poor quality of the XRT data, we can only infer a 2–10 keV flux of $\sim 8 \times 10^{-14}$ erg cm^{-2} s^{-1} by assuming a power law continuum (photon index frozen to 1.8) passing through the Galactic absorption ($N_{\rm H(Gal)} = 2.71 \times 10^{21}$ cm^{-2}).

None of the X–ray sources detected by XRT seem a plausible counterpart, unless the IBIS source is extremely variable.

IGR J23070+2203

(IBIS detection: 968.3–day outburst)

Three XRT observations available:

1. obscode: 00045407001
   observation date: 05/05/2011
   exposure: 893 s
2. obscode: 00045407002
   observation date: 08/05/2011
   exposure: 2144 s
3. obscode: 00045407003
   observation date: 14/05/2011
   exposure: 1286 s

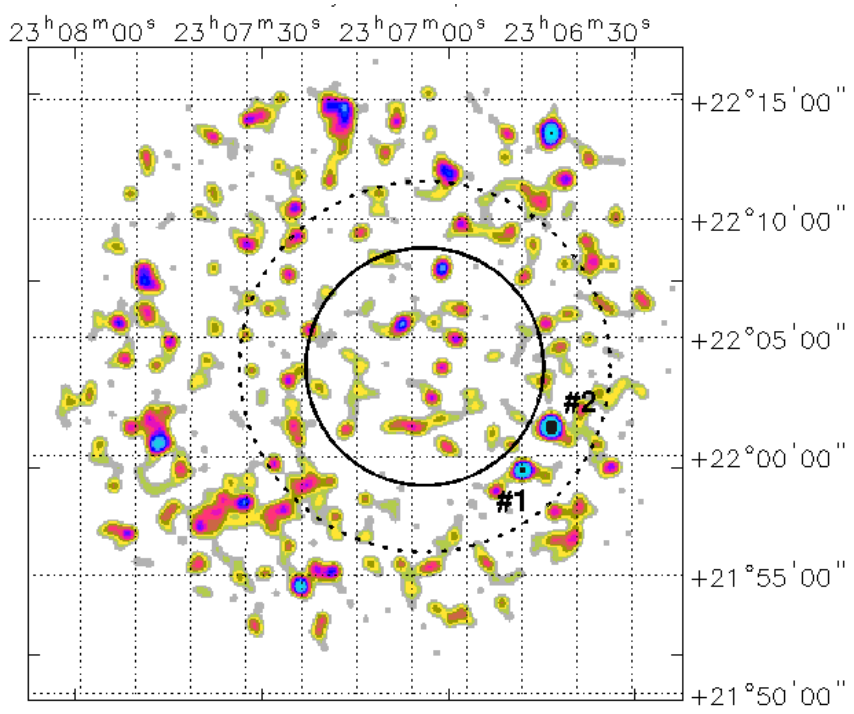

Figure 30: 0.3–10 keV XRT image of the IGR J23070+2203 field.

XRT detects two X–ray objects located within the 99% IBIS positional uncertainty:

➢ Source #1 is located at:

R.A.(J2000) = $23^h06^m39'.80$

Dec.(J2000) = $+21^{\circ}59'25''.30$

error box = $6''.00$

It is detected at 2.3σ c.l. in 0.3–10 keV energy band, and it is not visible above 3 keV.

Multi–wavelength counterparts to this XRT detection:

- WISE J230640.01+215929.2 with colours $W1 = 16.682 \pm 0.116$, $W2 = 16.027 \pm 0.212$, $W3 = 12.703 \pm 0.000$, and $W4 = 9.016 \pm 0.000$;
- 1SXPS J230639.7+215925.

➢ Source #2 is located at:

R.A.(J2000) = $23^{h}06^{m}34'.50$

Dec.(J2000) = $+22^{\circ}01'15''.70$

error box = $6''.00$

It is detected at 2.9σ c.l. in 0.3–10 keV energy band, and is not revealed above 3 keV.

Multi–wavelength counterparts to this XRT detection:

- USNO–A2.0 U1050.20564252 with magnitudes $R = 18.6$, and $B = 19.0$;
- WISE J230634.59+220120.3 with colours $W1 = 14.826 \pm 0.037$, $W2 = 13.948 \pm 0.045$, $W3 = 10.992 \pm 0.117$, and $W4 = 8.235 \pm 0.224$;
- *ROSAT* Faint source 1RXS J230634.6+220058 (20 arcseconds error radius);
- NVSS J230634+220122 (Flux(1.4 GHz) = 10.8 ± 0.5 mJy);
- 1SXPS J230634.3+220108 (coincident with the *ROSAT* source).

Bibliography

[1] Arabaci M. O., Kalemci E., Tomsick J. A., et al. 2012, ApJ, 761, 4

[2] Baumgartner W. H., Tueller J., Markwardt C. B., et al. 2013, ApJS, 207, 19

[3] Barentsen G., Farnhill H. J., Drew J. E., et al. 2014, MNRAS, 444, 3230

[4] Bianchi L., Herald J., Efremova B., et al. 2011, Ap&SS, 335, 161

[5] Bird A. J., Bazzano A., Bassani L., et al. 2010, ApJS, 186, 1

[6] Cavuoti S., Brescia M., D'Abrusco R., et al., 2012, MNRAS, 437, 968

[7] Chenevez J., Brandt S., Kuulkers E., et al. 2011, ATel 3183

[8] Condon J. J., Cotton W. D., Greisen E. W., et al. 1998, AJ, 115, 1693

[9] Evans P. A., Osborne J. P., Beardmore A. P., et al. 2014, ApJS, 210, 8

[10] Healey S. E., Romani R. W., Taylor G. B., et al. 2007, ApJS, 171, 61

[11] Kalberla P. M. W., Burton W. B., Hartmann D., et al. 2005, A&A, 440, 775

[12] Kozlowski S., Onken C. A., Kochanek C. S., et al. 2013, ApJ, 775, 92

[13] Landi R., Bassani L., Malizia A., et al. 2010, MNRAS, 403, 945

[14] Lucas P. W., Hoare M. G., Longmore A., et al. 2008, MNRAS, 391, 136

[15] Maiorano E., Landi R., Stephen J. B., et al. 2011, MNRAS, 416, 531

[16] Malizia A., Landi R., Bazzano A., et al. 2011, ATel #3391

[17] Masetti N., Parisi P., Palazzi E., et al. 2013, A&A, 556, A120

[18] Masetti N., Parisi P., Jimenez–Baiolon E., et al. 2012, A&A, 538, A123

[19] Masetti N., Parisi P., Palazzi E., et al. 2010, A&A, 519, A96

[20] Monet D. G., Levine S. E., Canzian B., et al. 2003, AJ, 125, 984

[21] Pickles A. & De Pagne E 2010, PASP, 122, 1437

[22] Puccetti S., Capalbi M., Giommi P., et al. 2011, A&A, 528, A122

[23] Rizzuto A. C., Ireland M. J., Kraus A. L. 2014, MNRAS, 448, 2737

[24] Rodriguez J., Bodaghee A., Tomsick J. A., 2010, ATel, 2557

[25] Saxton R. D., Read A. M., Esquej P., et al. 2008, A&A, 480, 611

[26] Skrutskie M. F., Cutri R. M., Stiening R., et al. 2006, AJ, 131, 1163

[27] Voges W., Aschenbach B., Boller Th., et al. 1999, A&A, 349, 389

[28] Watson et al. 2013, in prep

[29] Wright E. L., Eisenhardt P. R. M., Mainzer A. K., et al. 2010, AJ, 140, 1868